SSC-68

The Superconducting Super Collider

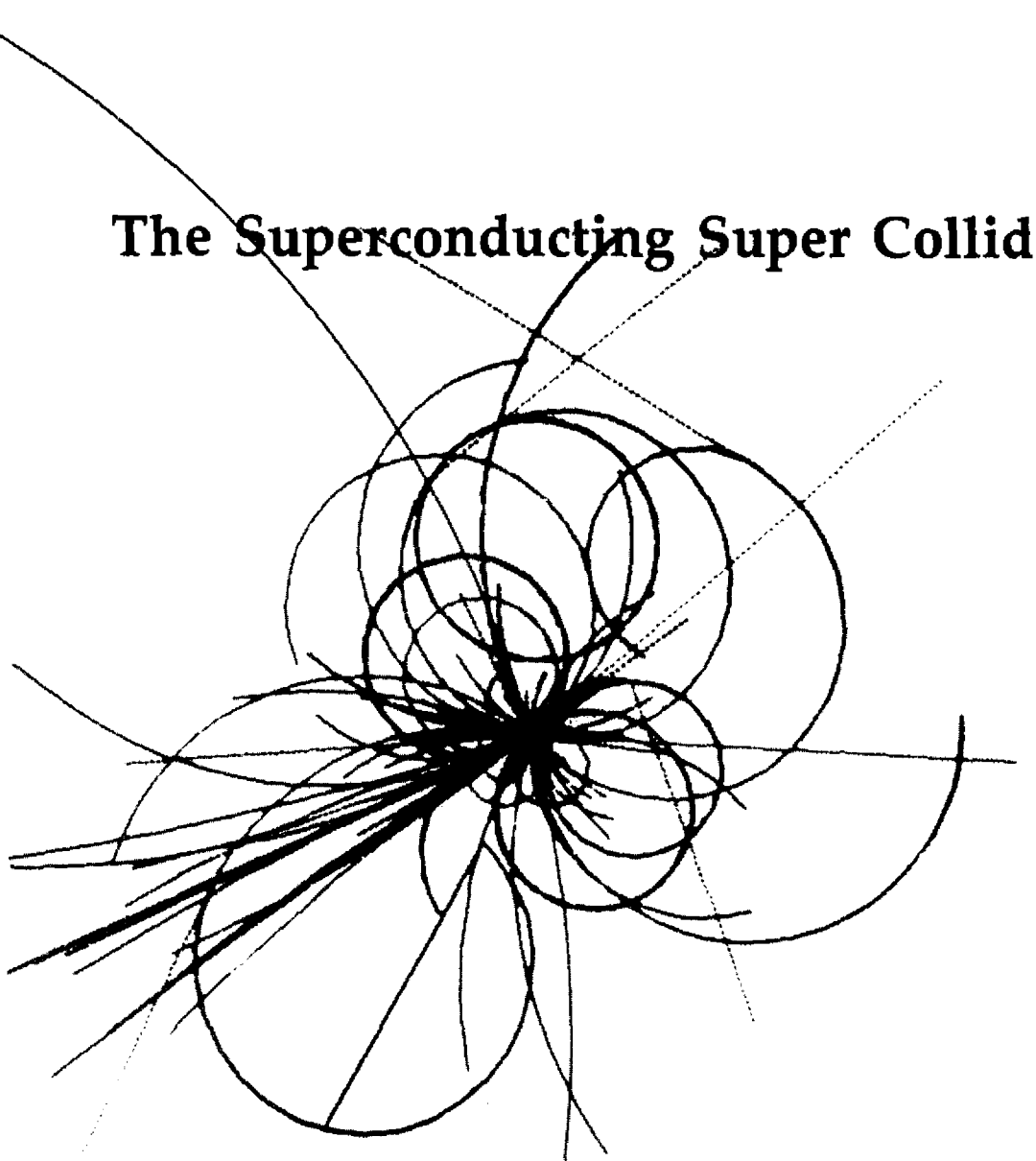

Comparison of Various Clustered Interaction Regions with Regard to Chromatic and Dynamic Behavior

B. Leemann and A. Wrulich
SSC Central Design Group

May 1986

SSC-68

COMPARISON OF VARIOUS CLUSTERED INTERACTION REGIONS WITH REGARD TO CHROMATIC AND DYNAMIC BEHAVIOR*

B. Leemann and A. Wrulich
SSC Central Design Group
c/o Lawrence Berkeley Laboratory
Berkeley, California 94720

May 1986

*Operated by Universities Research Association, Inc. for the U. S. Department of Energy

Comparison of Various Clustered Interaction Regions with Regard to Chromatic and Dynamic Behavior

B. Leemann and A. Wrulich

May 1986

1. Introduction

Clustered interaction regions for the SSC may be preferable from the viewpoint of costs and operation. In going from distributed to clustered IR's the superperiodicity of the machine is reduced and therefore the number of resonances induced by chromaticity correcting sextupoles is increased. This break in symmetry may cause a reduction in dynamic stability.

In chapter I the chromatic and dynamic behavior of the bare lattice is investigated for various cluster configurations. That means only chromaticity correcting sextupoles have been included and no magnetic imperfection errors have been considered. In chapter II the dynamic apertures of lattices with various IR clustering schemes are compared when random magnetic imperfections are included.

The dynamic aperture was found by tracking. It can only serve as a quality parameter for comparison between the distributed and clustered arrangements as long as the realistic lattice with imperfection errors included is not dominating the dynamic behavior. Although methods may be developed for reducing magnet errors it is unlikely that this will result in an increase in dynamic acceptance to the limit where lattice sextupoles will have noticeable influence.

The more important quality parameter is the chromatic behavior, that means the momentum dependence of tunes and betavalues at the interaction point, which is dominated by sextupoles of the bare lattice.

Following the Reference Design Study it was assumed that the lattice must provide 6 interaction regions. There are essentially three different ways of grouping six interaction regions in clusters and keeping the highest possible symmetry:

1. Two equally spaced 3-IR clusters ("3+3")
2. Three equally spaced 2-IR clusters ("2+2+2')
3. 4-IR cluster and at the diametrically opposite side a 2-IR cluster with 2 utility sections ("4+2")

2. Dynamic and Chromatic Properties of the Bare Lattice with Clustered Interaction Regions

For cluster configuration 1 and 2 the following sextupole arrangements were compared with respect to dynamical aperture and variation of tunes (Q_x, Q_z) and interaction beta values (β^*_y, β^*_z) with momentum:

- global correction scheme, i.e. 2 families of sextupoles with equal strengths for each family
- local interleaved correction
- local noninterleaved correction

For the two local correction schemes the sextupoles in the regular arcs were tuned to compensate the local cell chromaticity only. A lattice optics with approximately n + 1/4 phase advance between two interaction points was used.

2.1 Cluster Configuration "3 + 3"

Figures 1 and 2 show the variation of tune with momentum for the sextupole distribution C3.G (global), C3.LI (local interleaved) and C3.LN (local noninterleaved).

For the two local correction schemes only sextupoles between the two outer interaction points were used (6 1/2 cells). Since the tune advance between

2 IP's is n + 1/4, the linear beta variation with momentum produced by sextupoles is locally compensated within the cluster.

To avoid large sextupole strengths, for the local interleaved compensation both drift spaces left and right from a cell quadrupole were equipped with sextupoles.

The variation of horizontal and vertical interaction beta with momentum for the inner and outer interaction points of the cluster are shown in Figures 3 to 6.

Figure 7 shows the variation of dynamical aperture (i.e. maximum horizontal amplitude for 100% emittance coupling) with momentum.

The tracking was performed for 4 different initial conditions (x, x', z, z') = ($\hat{x}$, 0, $\hat{z}$, 0), (-$\hat{x}$, 0, $\hat{z}$, 0), ($\hat{x}$, 0, 0, $\hat{z}'$), and (-$\hat{x}$, 0, 0, $\hat{z}'$) over 50 revolutions.

2.2 Cluster Configuration "2 + 2 + 2"

To achieve a cancellation of the linear beta beat produced by sextupoles, in the local correction schemes a corresponding number of cells outside the cluster was added for the local correction, so that the arrangement got the following structure:

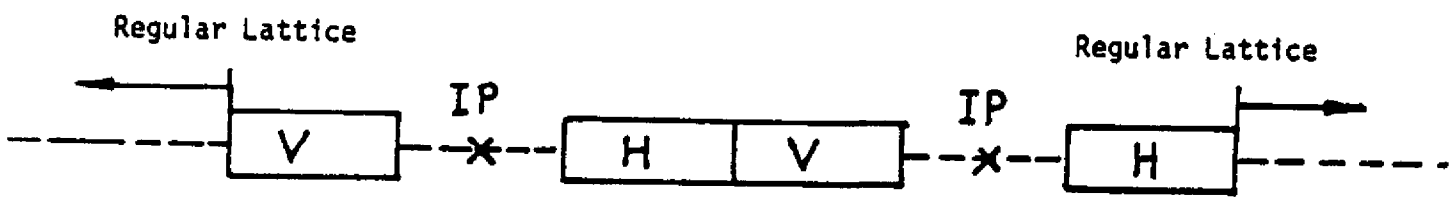

For the local noninterleaved compensation one pair of sextupole was used in each section V and H.

Figures 8 and 9 show the variation of horizontal tune and β^* with momentum. Due to symmetry reasons both interaction points in the cluster show the same β-variation. Even tune and beta variation in both planes are equal, as shown in Figures 10 and 11. The slight difference between the two planes is a result of the difference in tune (Q_x = 85.265/Q_z = 85.285).

Figure 12 shows the variation of dynamic aperture with momentum. The symmetric behavior of the global compensation (C2.G) is caused by a drastic increase of the $2Q_x$-$2Q_z$ driving term for positive momentum deviation.

Figure 13 shows the variation of 2 different tunes with momentum. For both cases the dynamical aperture is reduced for positive momentum deviation as shown in Figure 12. That means a change of the resonance driving term has caused the loss in stability and not a shift of the tune onto a resonance as a result of the momentum variation.

A motion of the tune away from the coupling resonance $2Q_x$-$2Q_z$, should bring an increase in stable amplitude for positive momentum deviation.

3. Comparison of Sextupole Compensation Schemes

3.1 Nonlinerleaved/Interleaved

For the noninterleaved distribution the dynamical aperture is extremely large for small energy deviations. Even for the tails of the energy distribution it is sufficiently large.

But orbit errors (i.e. focusing errors due to orbit displacements in the sextupoles), sextupole displacement errors and quadrupole errors have not been taken into account yet. The noninterleaved distribution tend to be very sensitive to these errors.

On the other hand also the momentum dependence of tunes and interaction betas are intolerably large and it is difficult to compensate them (by introducing more sextupole families).

3.2 Global Compensation Local Compensation

An acceptable sextupole distribution should provide

- large dynamical aperture
- small variation of tune with momentum
- small variation of β^* with momentum

All local compensations in the examples given above are clearly worse than the global distributions. For the specific examples there is no preference for the local sextupole compensation.

3.3 Cluster configuration "4 + 2"

The 4-2 configuration combined with utility sections is the most preferable for site layout. The results for the cluster configurations 1 and 2 clearly show that a global interleaved sextupole distribution gives the best results and was adopted therefore for all further considerations.

Three different examples for the 4-2 configuration have been investigated:

3.3.1 "XXXX-UXXU" - type with $\Delta Q(IR-IR) = 0.71$

The interaction regions of the 2-IR cluster are placed symmetrically around the symmetry point and the utility sections are located outside; the phase advance between two adjacent IR's is $2\pi * 0.71$.

3.3.2 "XXXX-UUXX" - type with $\Delta Q(IR-IR) = 0.71$

Interaction region and utility sections are grouped in pairs around the symmetry point.

3.3.3 "XXXX-UUXX" - type with $\Delta Q(IR-IR) = 0.75$

the phase advance is set to its optimum value for compensating the momentum dependent beta beat.

For all three types of cluster configurations the variation of betavalue at the interaction point with momentum is shown in Figures 14, 15, 16. Only the weakest and most pronounced variation out of all 6 interaction points are drawn there. Due to symmetry reasons the beta values in the orthogonal plane must have the same behavior and are therefore not explicitly shown here.

Figure 17 shows the momentum dependence of horizontal tune, and Fig. 18 correspondingly the variation of vertical tune.

The maximum stable amplitude for all three configurations is shown in Fig. 19. The amplitudes drawn for the interaction point with beta-x = beta-z = 1.0 m. Tracking was performed for 4 particles over 400 turns.

The maximum deviations of tune and $(\frac{\Delta\beta}{\beta})/(\frac{\Delta p}{p})$ over the momentum range of ± 0.001, the minimum stable amplitude are compared in the following table for all configurations:

3.4. Comparison of Dynamic Behavior

The dynamic acceptance is significantly larger for the cluster configuration with higher symmetry ("2+2+2"). all other cluster with 2-fold symmetry only, have stable amplitudes in approximately the same range. But as already mentioned before,, the dynamic behavior is dominated by imperfection errors which reduce the stable amplitude considerably below the limits shown here.

3.5 Comparison of Chromatic Behavior

The configuration with 3 cluster per circumference is also noticeable superior in the chromatic behavior. The momentum dependence of tune and beta* are considerably weaker.

The configuration with 3 IR's per cluster ("3+3") is worse than clusters with interaction regions grouped in pairs. For the 3-IR arrangements the linear off momentum beta cannot be compensated within one cluster if at the

same time the momentum dependence of beta value at all three interaction points within the cluster should be minimum.

For the compensation effect of the linear momentum dependence of beta value the phase advance between the interaction points is important and must be appropriately chosen as an odd multiple of one quarter wave length. this result becomes evident by comparing the cluster configuration "XXX-XXUU" for two different tune advances, i.e. $\Delta Q(IR-IR) \approx 0.71$ and 0.75.

A symmetric arrangement of the two interaction regions in the 4-2 configuration is preferable, as can be seen by comparing the structures "XXXX-XXUU" and "XXXX-XUUX"). This configuration would possibly permit injection both rings from a booster with protons circulating in one direction only.

4. Dynamic Aperture for Lattices with Various IR Clustering Configurations Including Random Magnet Imperfections

This part of the report is a summary of tracking studies on non-linear lattices performed during the second half of 1985 at the SSC/CDG. In this period the lattice design was characterized by the exploration of IR clustering configurations and the transition from test lattices (no beam crossings , no utility insertions) to realistic lattices. This evolution manifests itself in the tracking data reported here through occasional discontinuities in the parameter sets used and caution is indicated when comparing results.

4.1 Tracking

All the tracking results reported here were obtained using the code "PATRICIA" and including the random multipole moments of dipole magnets only . The actual values are insignificantly different from the RMS values for magnet design "D" (4 cm coil diameter) with 9μ filament size*, except for the random

quadrupole moments $\sigma_{a,1}$, $\sigma_{b,1}$, which have been set to zero in order to suppress the resulting tune shift and linear coupling. The values used are listed in table 2 .

The dynamic aperture is determined by the maximum initial amplitudes x = y for which a particle survives 400 revolutions. The tracking point is always one of the interaction points and

$$(a^*_{dyn})^2 = (x^*)^2 + (y^*)^2$$

For each lattice the dynamic aperture is determined for 5 random number seeds for 3 $\Delta p/p$ cases : on-momentum, $\delta = 0$ and 2 symmetric off-momentum values, $\pm\,\delta$. For one random number seed a momentum scan of the dynamic aperture is performed in the range $\pm\,2\times10^{-3}$.

4.2 Dynamic Aperture of Distributed IR Lattice "TLD1"

The test lattice TLD1 has been investigated extensively. It has superperiodicity 6 and therefore no utility insertions. The dynamic aperture as a function of $\Delta p/p$ is shown in Fig. 20 and may serve as the basis for the comparison of the dynamic aperture of the clustered IR lattices.

4.3 Dynamic Aperture of the "3+3" Clustering Configuration TLD133

As in the case of the distributed lattice TLD1 the TLD133 does not have any utility insertions. The phase advance between 2 IP's is not quite n±1/4, required for local compensation within the cluster of the linear beta variations with momentum produced by sextupoles. The fractional change in phase between adjacent IR's is $\Delta Q = .71$.

---

* "Magnetic Errors in the SSC", SSC-7 , April 1985

Fig. 21 shows the dynamic aperture for the "3+3" clustering configuration with a global 2 family sextupole chromaticity correction scheme. For $\delta = 0$, $\pm 1.5\times10^{-3}$ the dynamic aperture has been determined for 5 random number seeds, indicated by different symbols. For one of these seeds a momentum scan produced the dynamic aperture within the momentum range of $\pm 2\times10^{-3}$.

Roughly speaking the IR's contribute about one half to the total natural chromaticity of the lattice. By using the sextupoles in the 6&1/2 cells between adjacent IP's as a local interleaved sextupole correction scheme one arrives at the configuration which is shown in Fig. 22. Though only performed for one random number seed, it is quite similar to the globally corrected configuration shown in Fig. 21. This underlines the fact that we are in a regime dominated by magnet imperfections rather than by lattice sextupoles.

An interesting fact is that the maximum value of the dynamic aperture hardly depends on the random number seed, but the $\Delta p/p$ value for which it occurs is definitely seed dependent. Therefore the standard deviation of the average dynamic aperture as based on the 5 samples at $d = 0$ will overestimate the variation of the on-momentum dynamic aperture.

While the dynamic aperture of the distributed IR case is flat over a wider momentum range, the dynamic aperture of the clustered configuration "3+3" is larger over the range of interest $\pm1\times10^{-3}$ for $\Delta p/p$.

4.4 Dynamic Aperture of the "4+2" Clustering Configuration in TLD124A & TLD124B

The lattice TLD124A corresponds to what was referred to in chapter I as "XXXX-UXXU" configuration, while TLD124B corresponds to "XXXX-UUXX". New for the lattices of the type TLD124 is that they include pseudo-utility insertions, made up of 6&1/2 regular cells (without dipole magnets) sandwiched between pairs of phase trombones and dispersion suppressors. Besides having different placements of the utilities TLD124A has a fractional

phase advance between adjacent IP's of .71, while TLD124B has complete compensation of the linear beta wave by having $\Delta Q = n \pm 1/4$. The dynamic apertures for these two cases are given in Fig. 23 and Fig. 24. They are very similar with TLD124B having a few percent larger dynamic aperture, thanks to the 1/4 integer phase advance between IP's .

4.5 Summary and Conclusions

Dynamic and chromatic behavior of various IR-cluster arrangements with six interaction regions per ring have been investigated. configurations with interaction regions grouped in paris show significantly better chromatic behavior, if the phase advance between the interaction points is appropriately chosen as an odd multiple of one quarter wavelength.

The dynamic acceptance even for configurations with completely broken symmetry is far above the limitation given by magnet imperfection errors and is therefore of minor relevance for the selection process.

In addition, the dynamic aperture of lattices with various clustering configurations and with random magnet imperfections included have been explored. Though we are in a regime dominated by magnet imperfections, our results follow exactly the trend that was found for the linear lattices in Chapter I.

The dynamic apertures of clustered IR lattices with random magnet imperfections included favors configurations with pairs of insertions separated by a phase advance of $n \pm 1/4$. In this case the dynamic aperture appears to be 15 to 20% larger in the momentum range of 11×10^{-3} than for the lattice with distributed IR's .

Clustered IR's, if appropriately chosen, have no disadvantage as compared with distributed IR's.

Table 1.

Parameters for the Range $-.001<\Delta\rho/\rho<0.001$	3+3	2+2+2	ΔQ(IR-IR)=0.71	ΔQ=0.71	ΔQ=0.75	Units
$\left(\Delta Q_x \quad max\right)$	2.8×10^{-3}	1.8×10^{-3}	1.9×10^{-3}	3.5×10^{-3}	1.5×10^{-3}	
$\left(\Delta Q_z \quad max\right)$	2.9×10^{-3}	1.7×10^{-3}	1.7×10^{-3}	3.6×10^{-3}	1.4×10^{-3}	
$\left(\frac{\Delta\beta^*_x/\frac{\Delta\rho}{\rho}}{\beta_x} \quad max\right)$	10.2	2.8	7.1	17.9	7.0	[%]
$\left(\frac{\Delta\beta^*_z/\frac{\Delta\rho}{\rho}}{\beta_z} \quad max\right)$	9.6	2.9	6.1	15.7	6.3	[%]
(A_x) min	3.42	6.35	4.7	3.9	5.1	[mm]

Table 2*

RMS Multipole variations in units of 10^{-4} at 1 cm
an, bn = skew, normal coefficient of 2(n+1)-pole

n	$\sigma_{a,n}$	$\sigma_{b,n}$
2	2.14	.63
3	.69	.35
4	.59	.14
5	.059	.16
6	.078	.034
7	.016	.030
8	.021	.0064
9	.0030	.005
10	.0071	.0012

* "Magnetic Errors in the SSC", SSC-7, April 1985

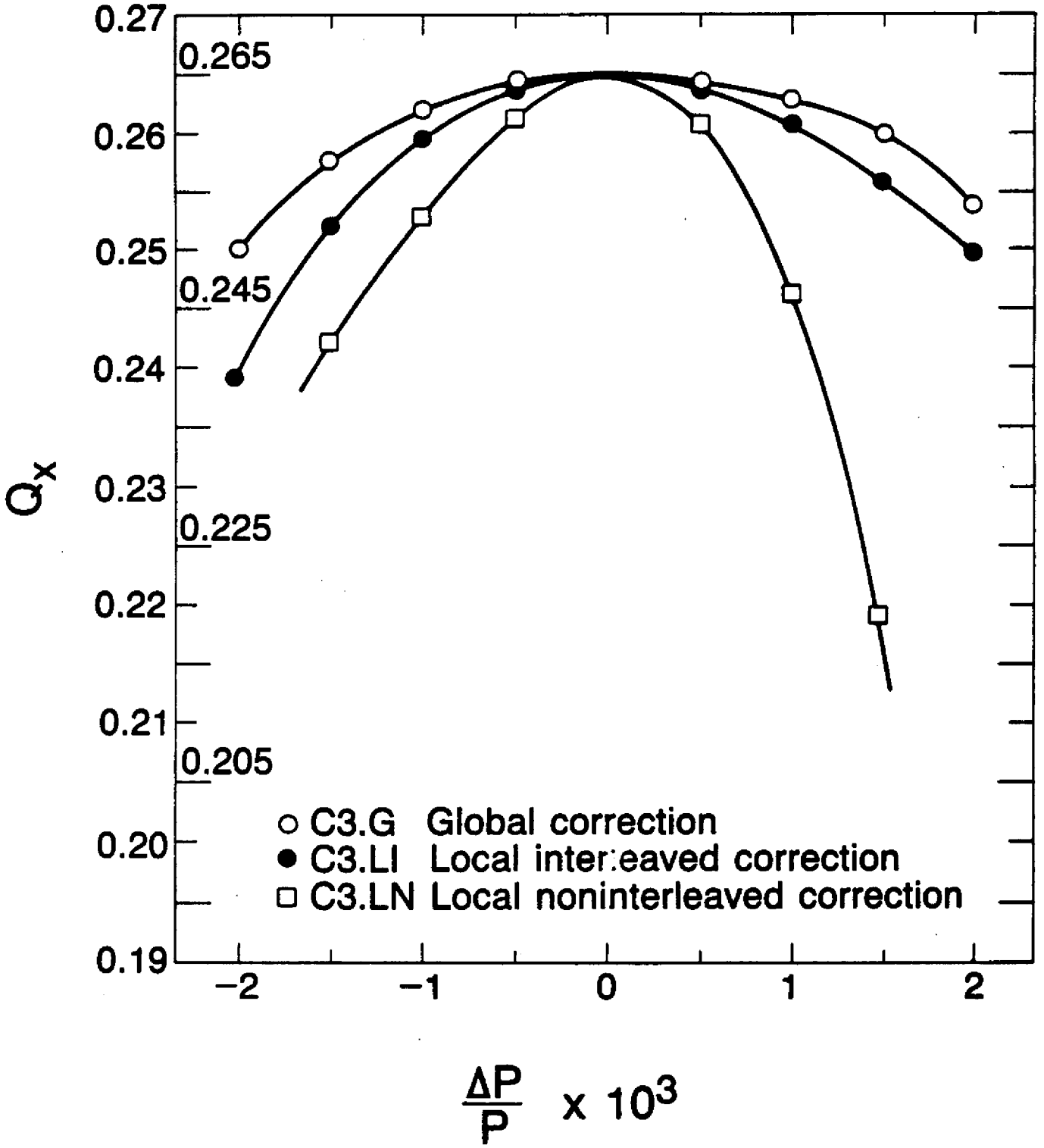

Figure 1. (3IR) Horizontal Tune vs. Momentum

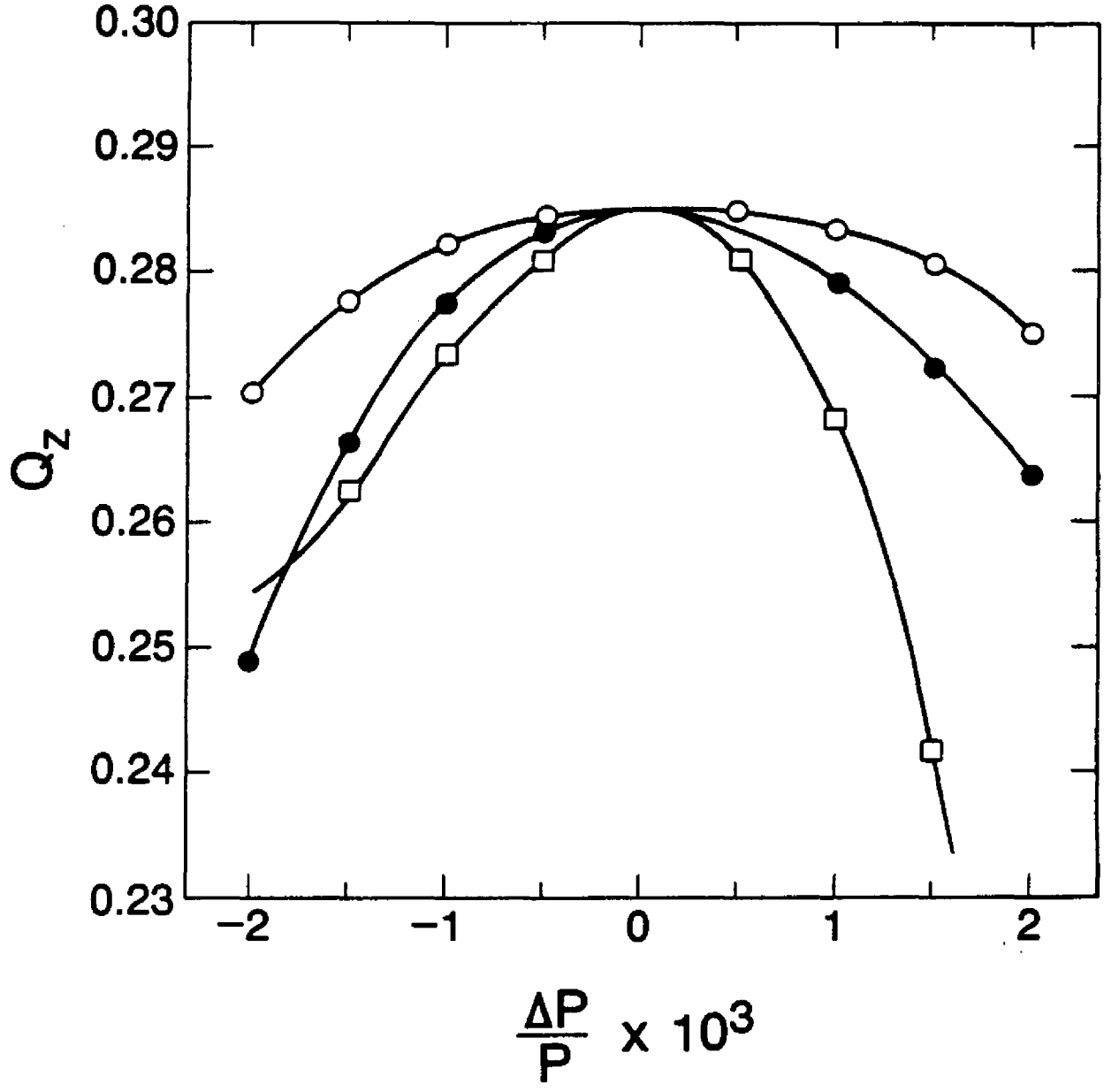

Figure 2. (3IR) Verticle Tune vs. Momentum

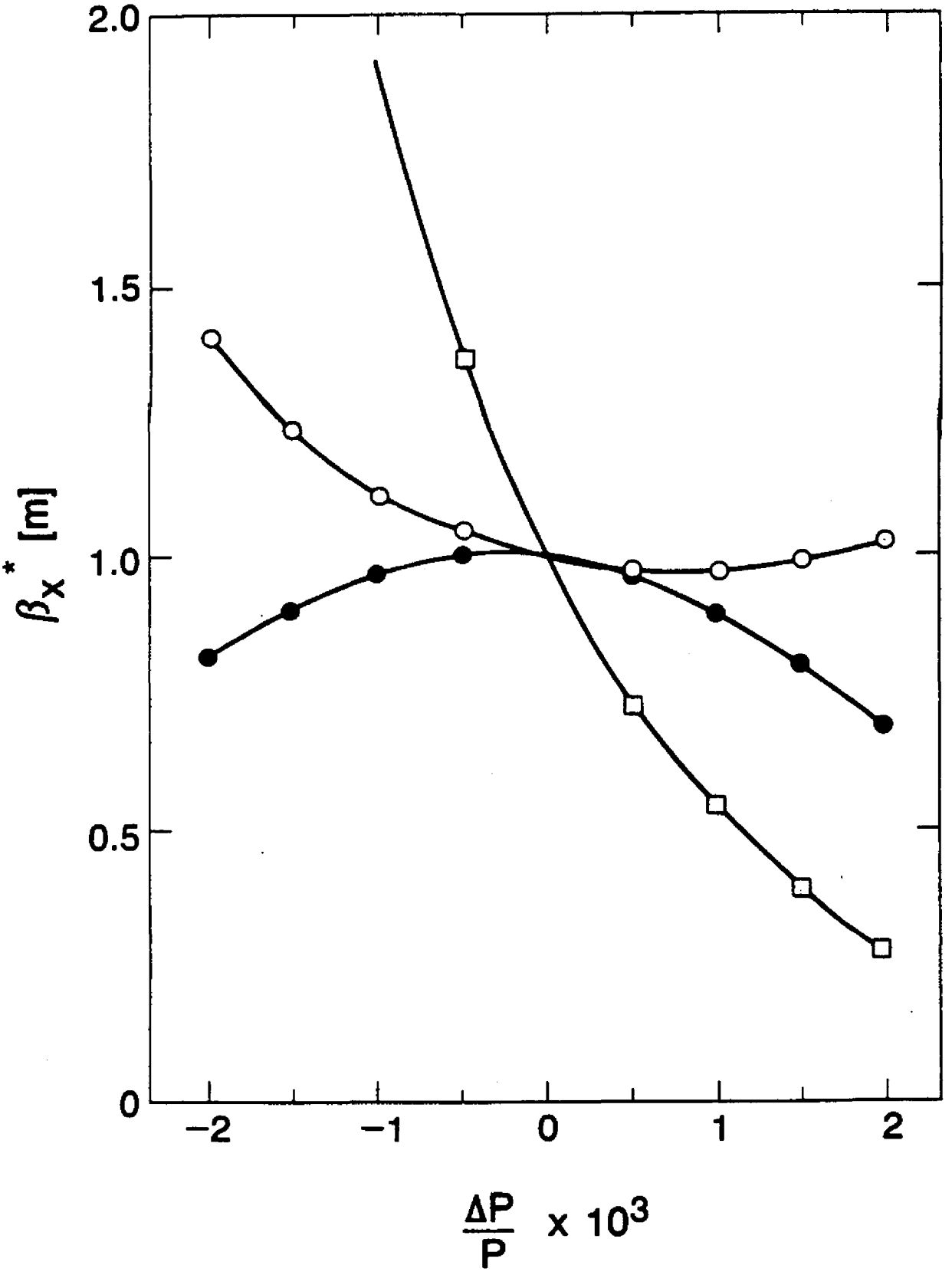

Figure 3. (3IR) β^*_x vs. Momentum

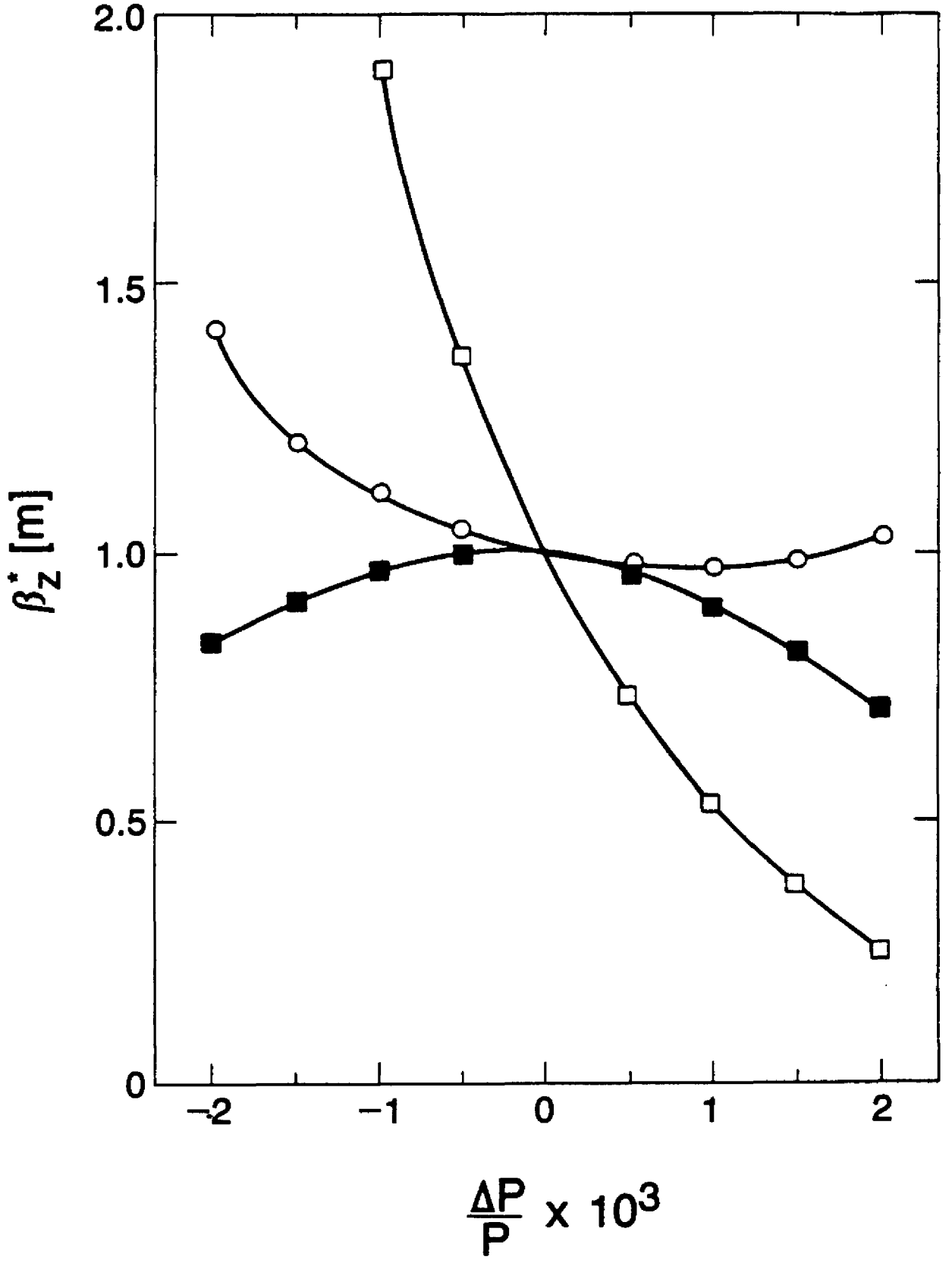

Figure 4. (3IR) β^*_z vs. Momentum

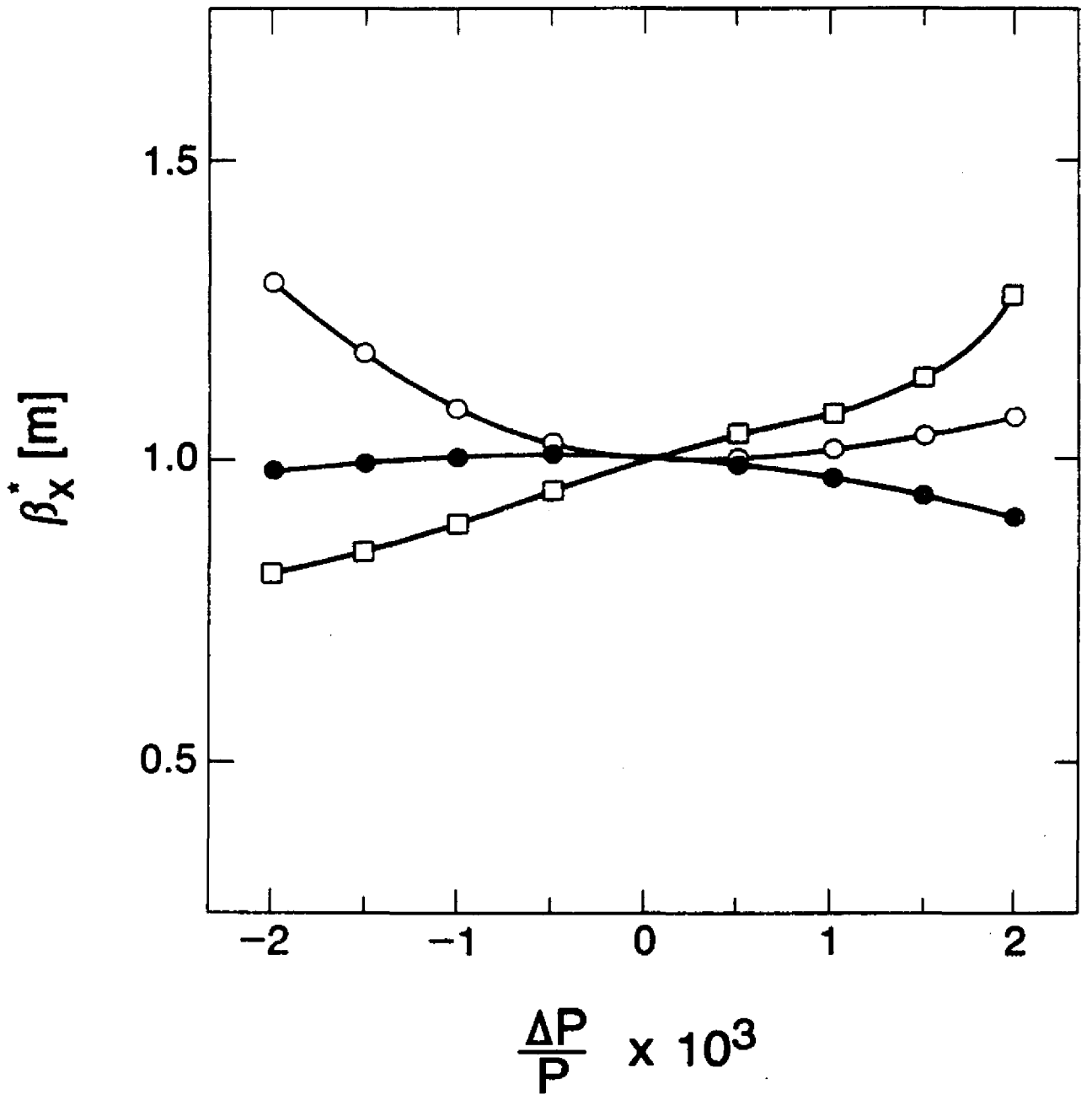

Figure 5. (3IR) β^*_x vs. Momentum

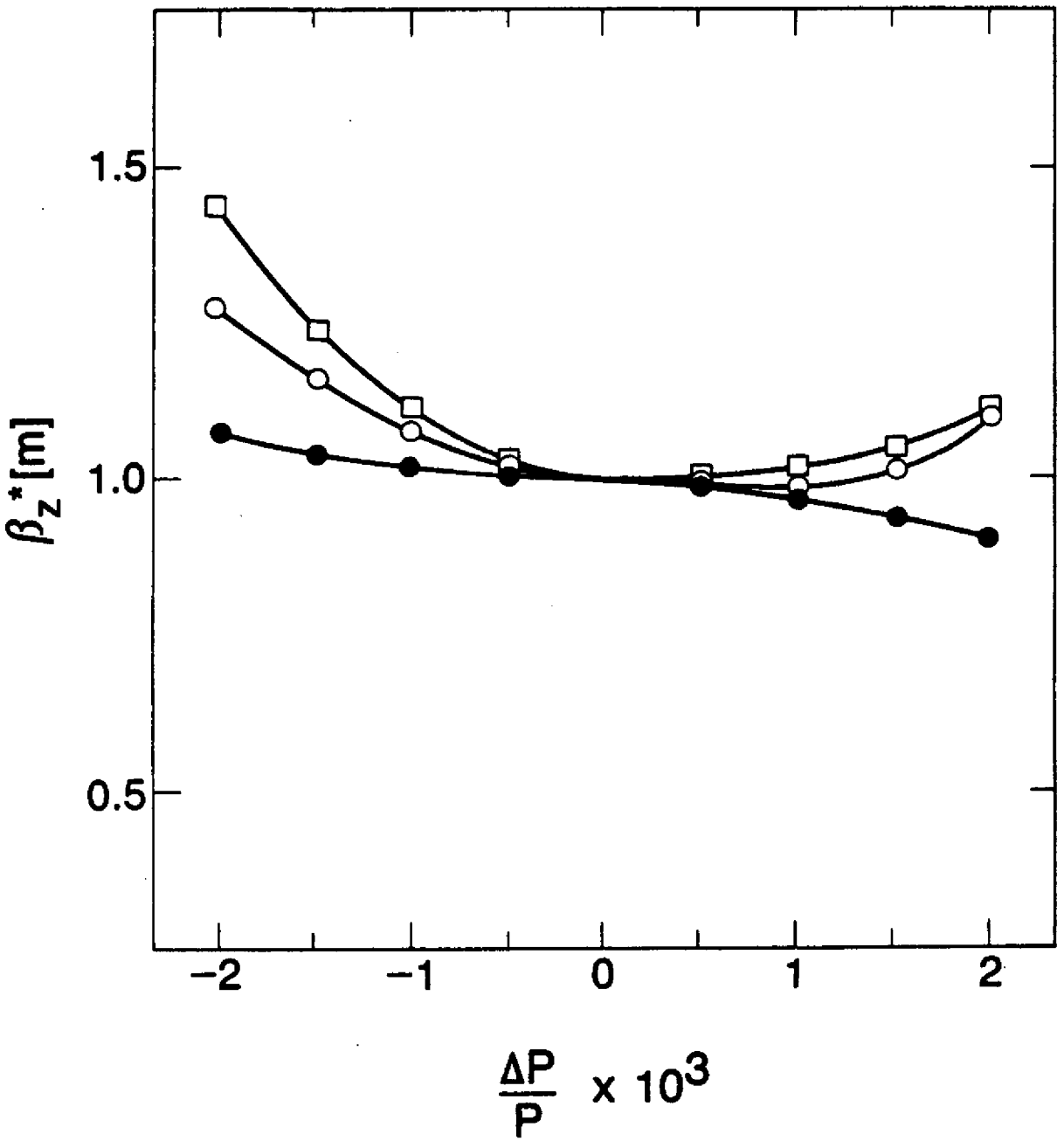

Figure 6. (3IR) β^*_z vs. Momentum

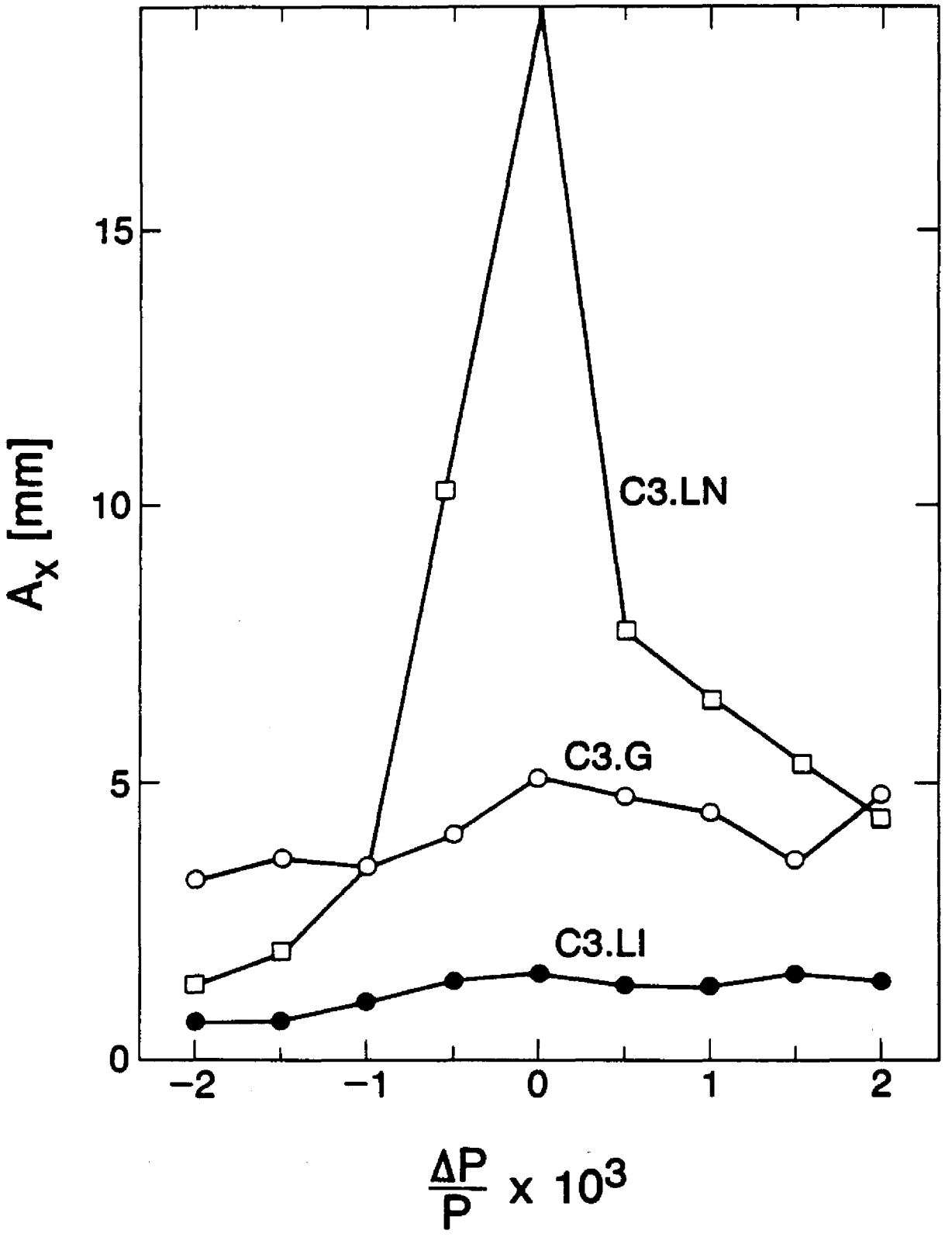

Figure 7. (3IR) Maximum Stable Horizontal Amplitude vs. Momentum

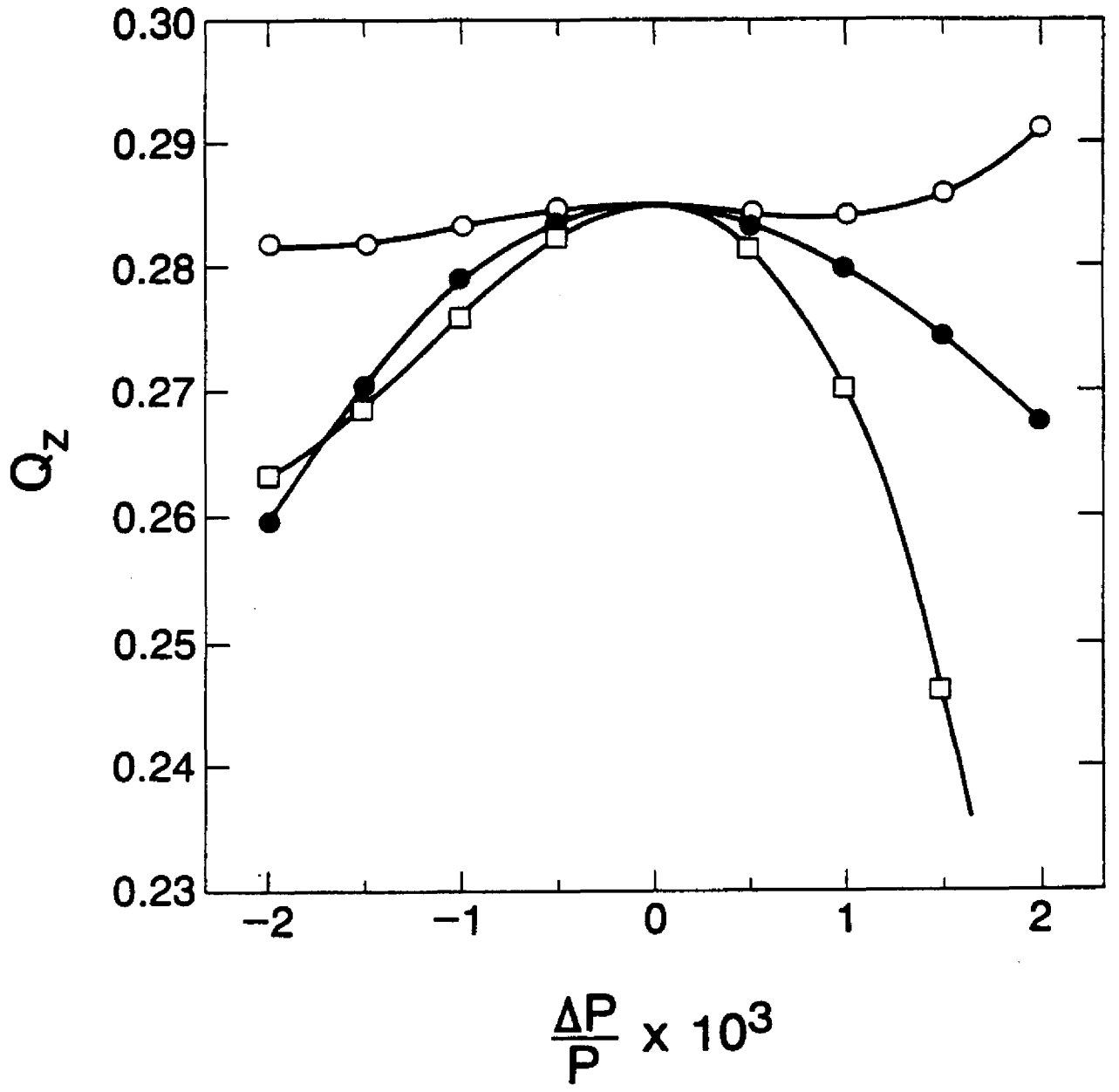

Figure 8. (2IR) Horizontal Tune vs. Momentum

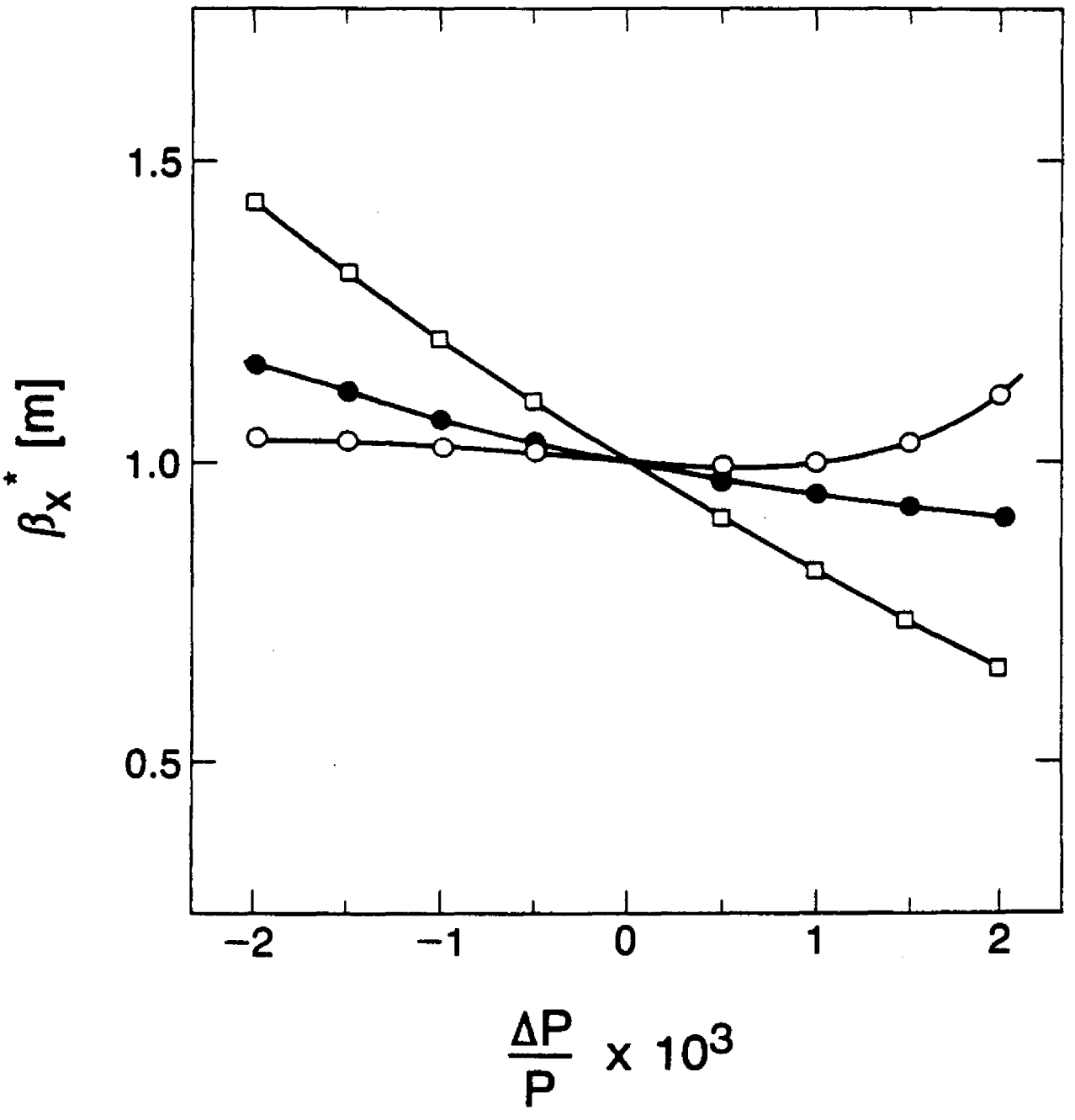

Figure 9. (2IR) β^*_x vs. Momentum

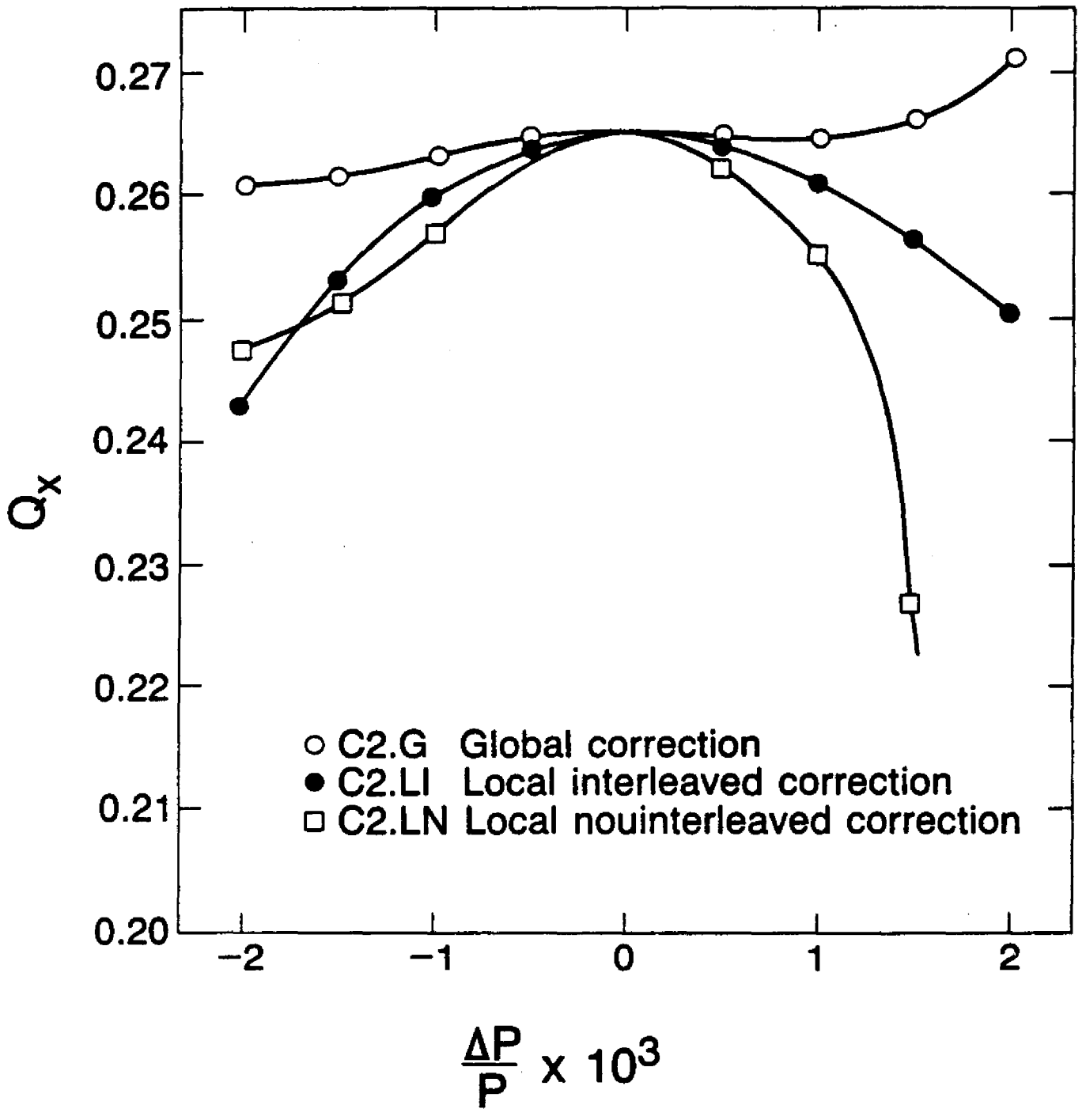

Figure 10. (2IR) Verticle Tune vs. Momentum

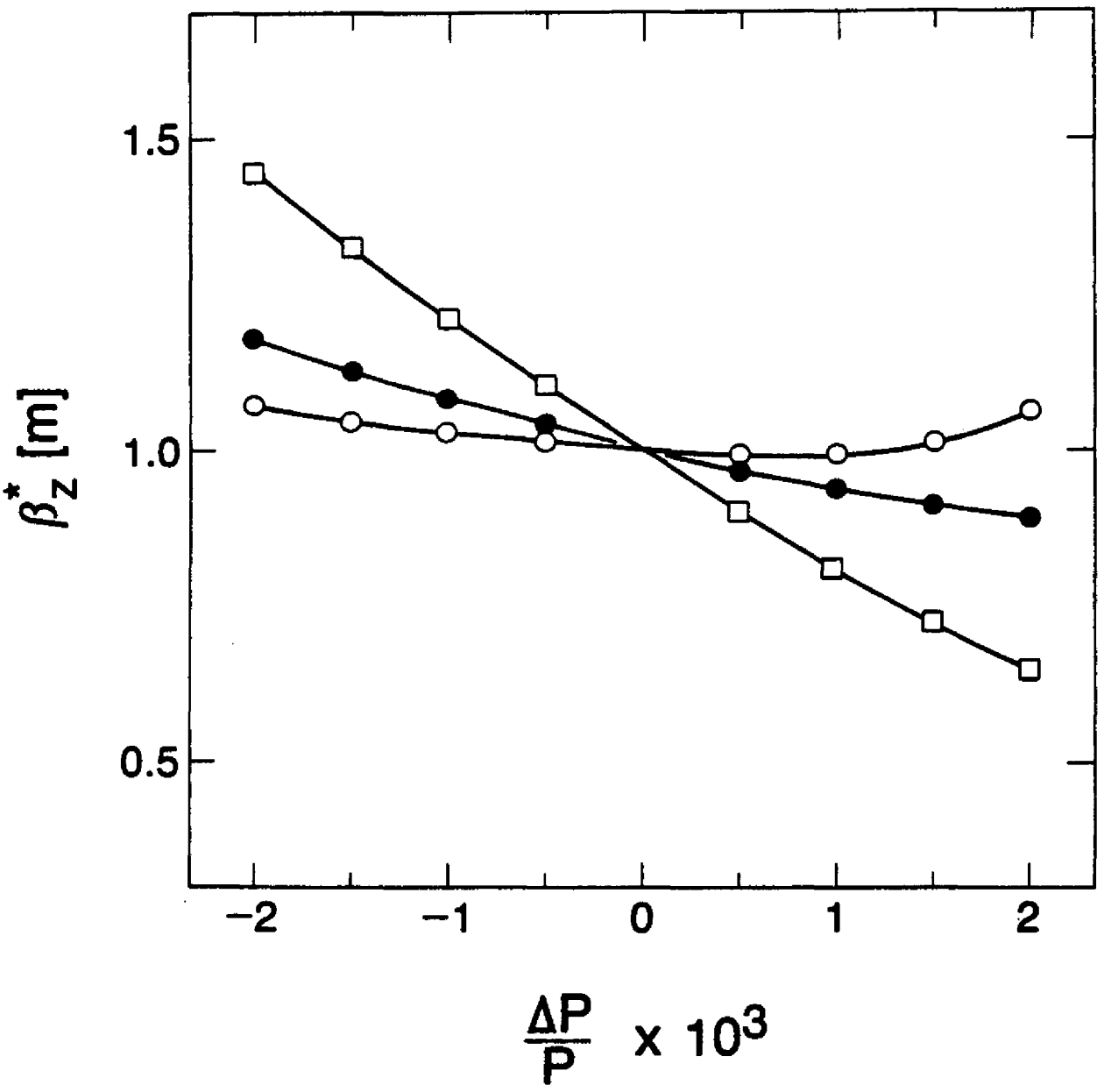

Figure 11. (2IR) β^*_z vs. Momentum

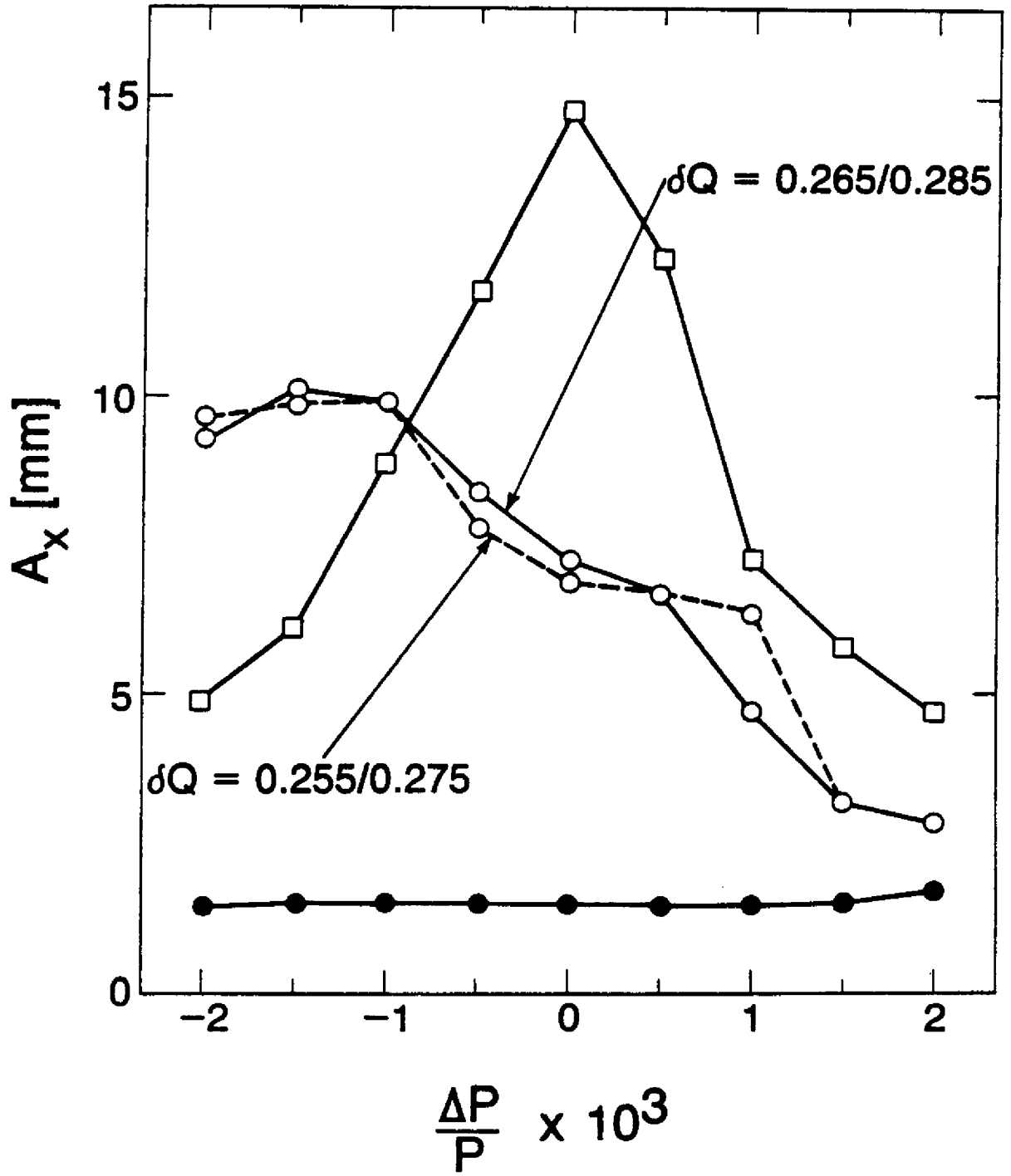

Figure 12. (2IR) Maximum Stable Horizontal Amplitude vs. Momentum

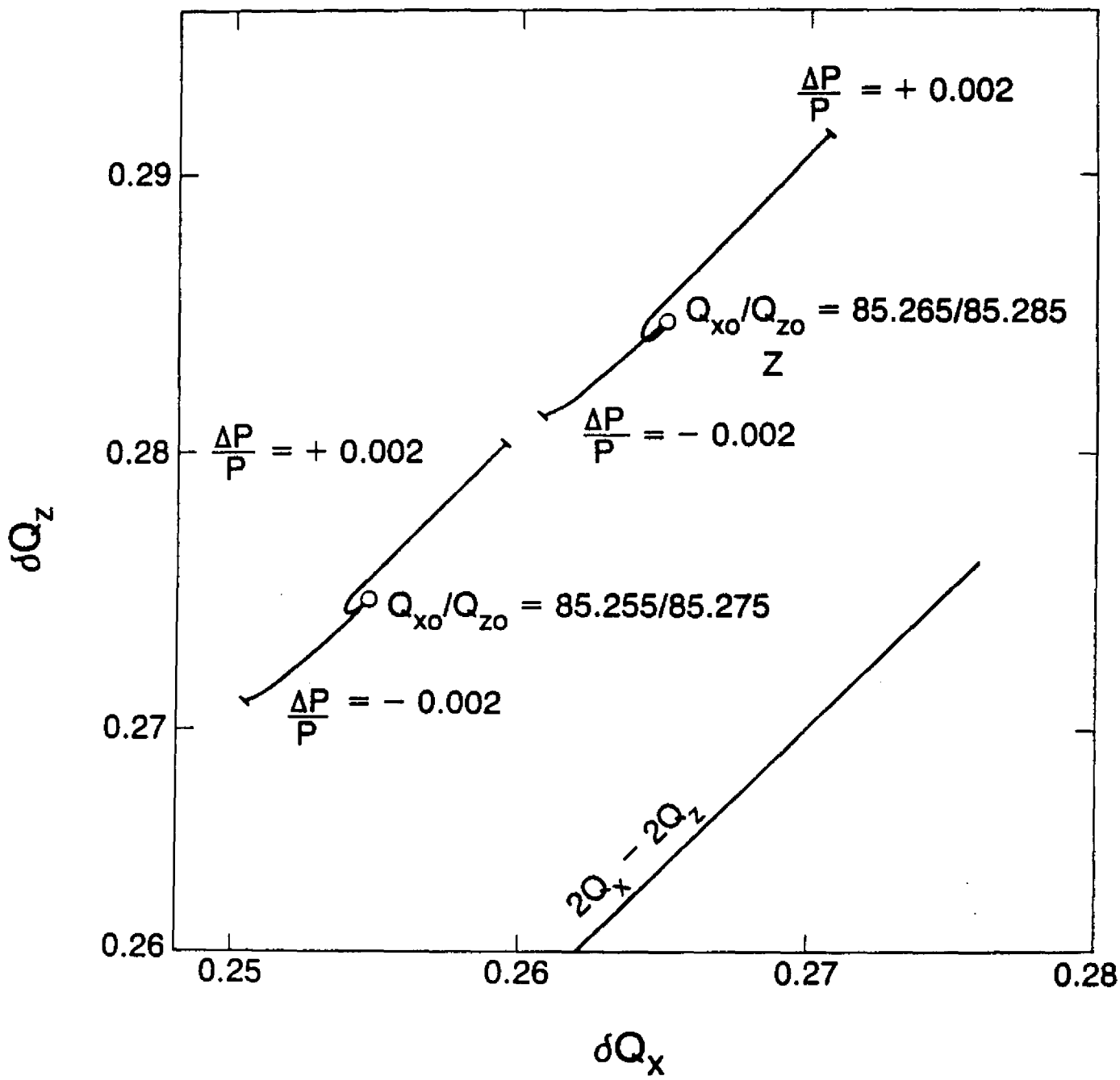

Figure 13. (2IR) Variation of Tune with Momentum

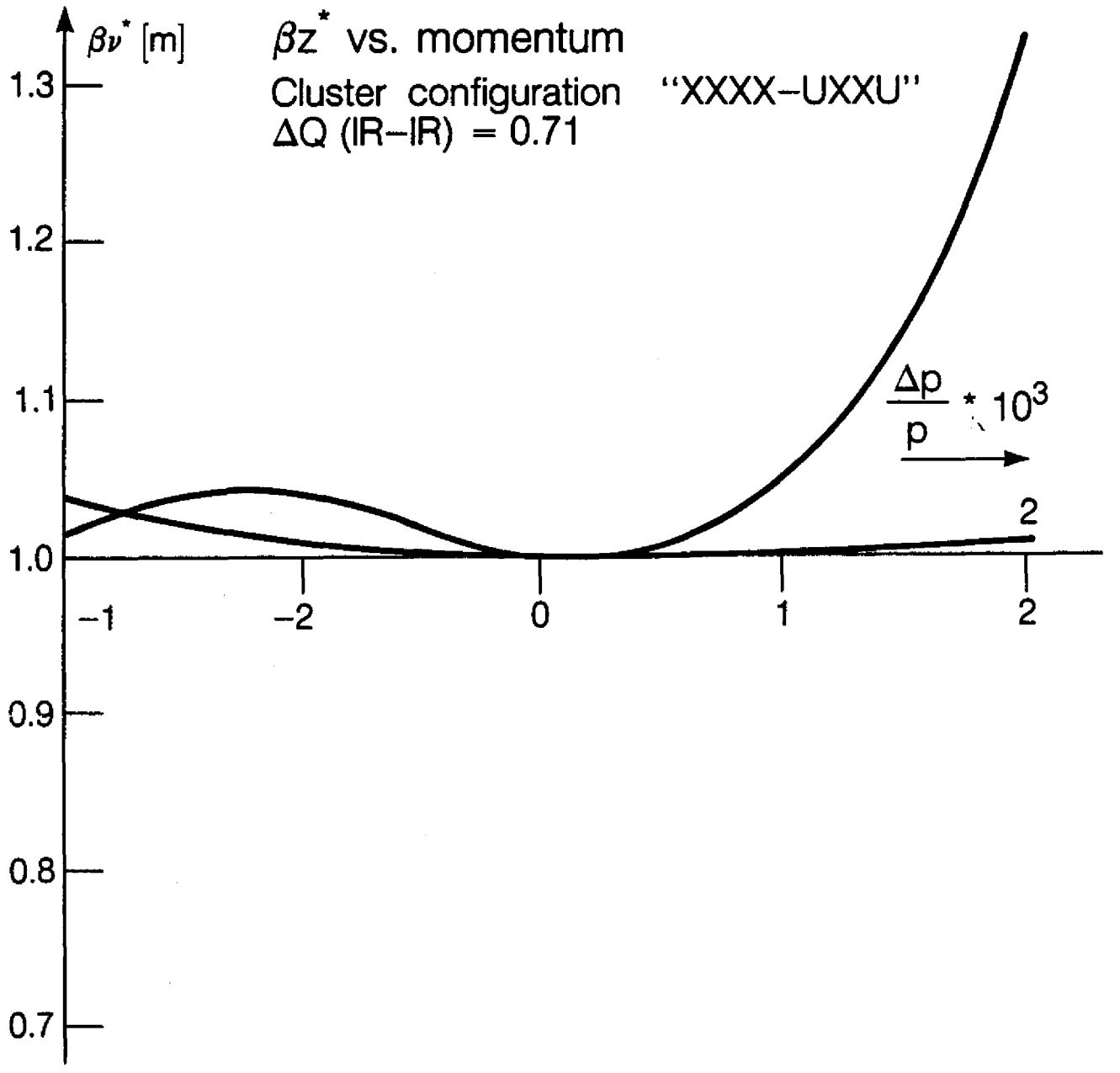

Figure 14. β^*_z vs. Momentum

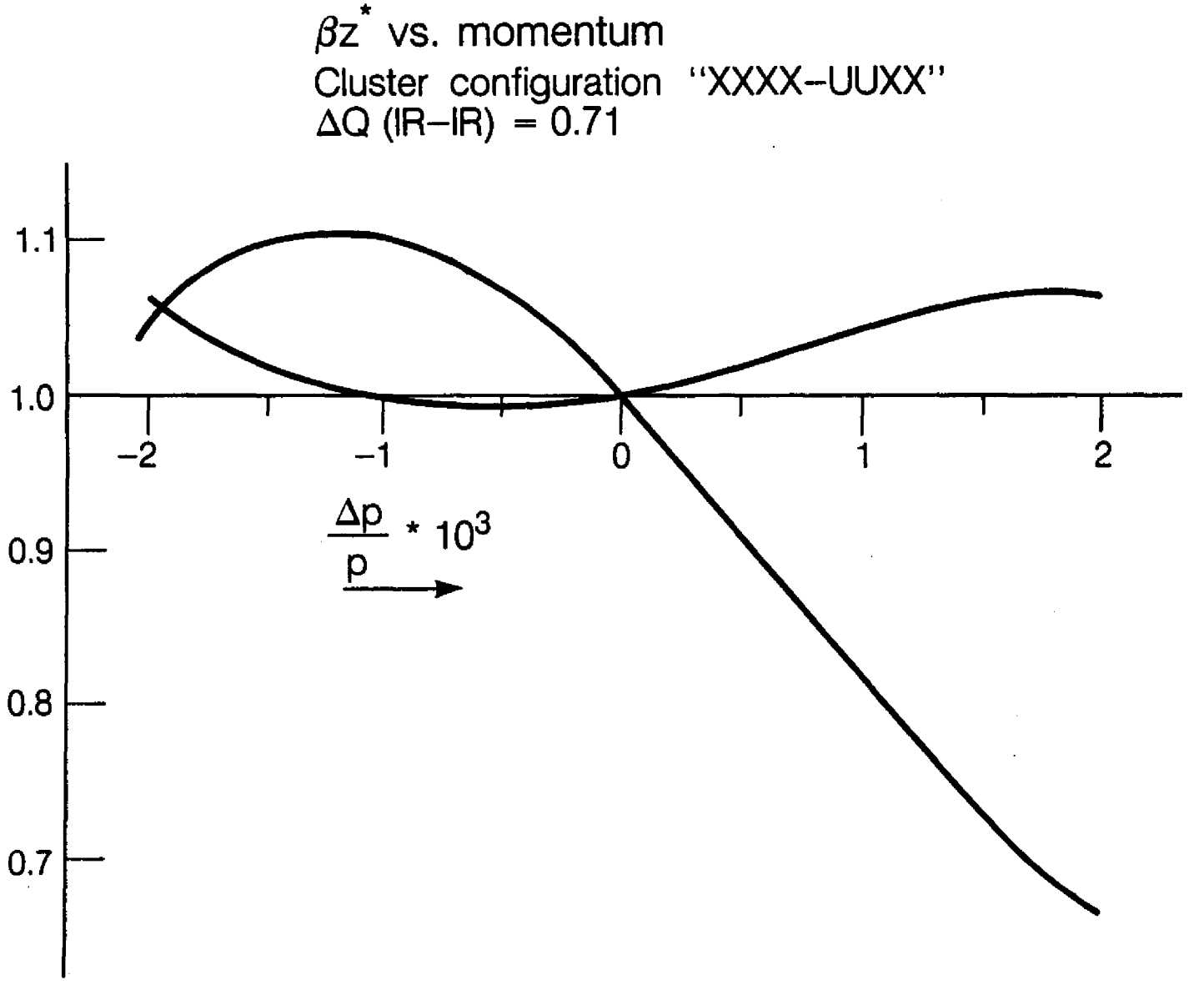

Figure 15. β^*_z vs. Momentum

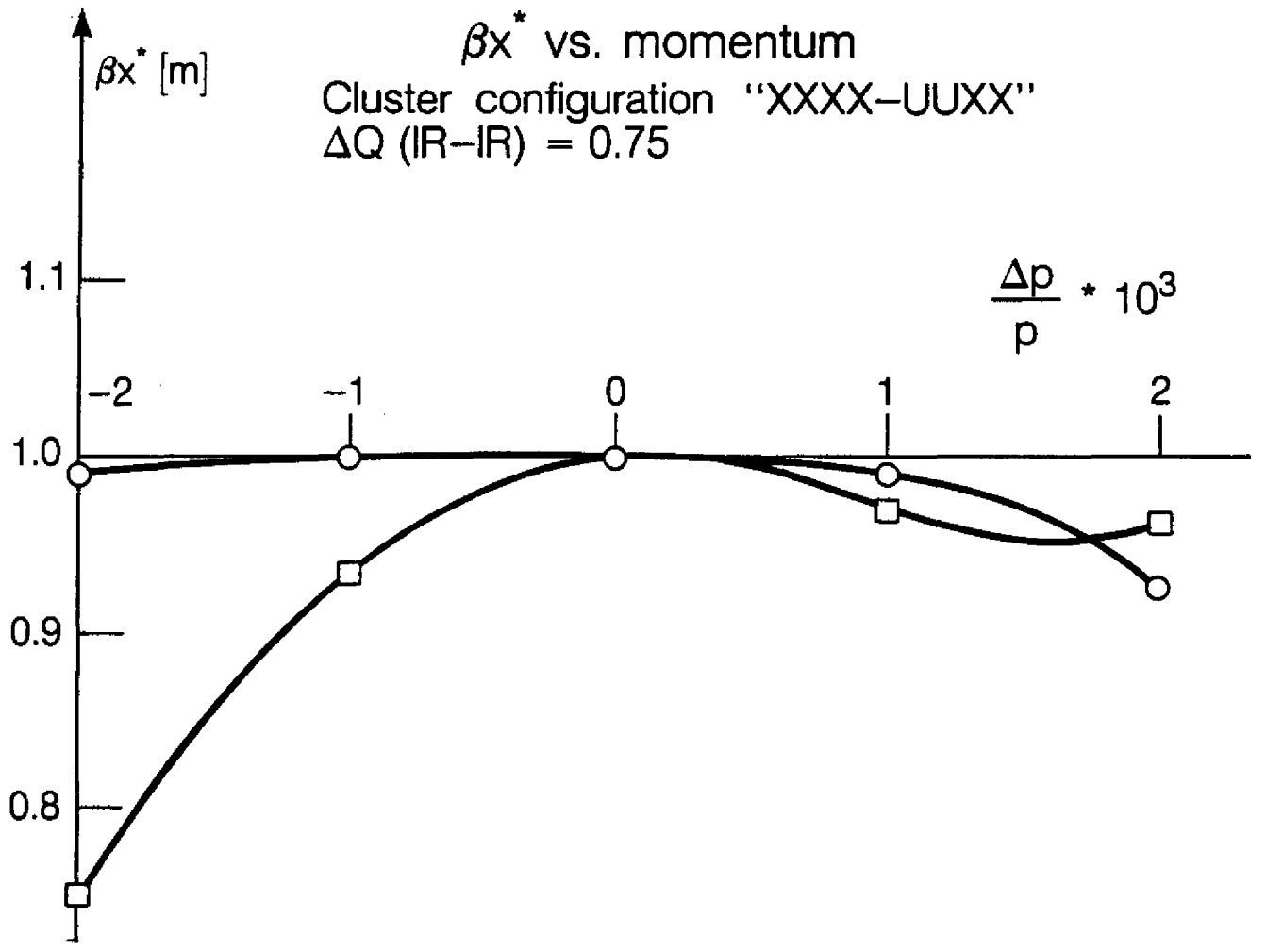

Figure 16. β^*_x vs. Momentum

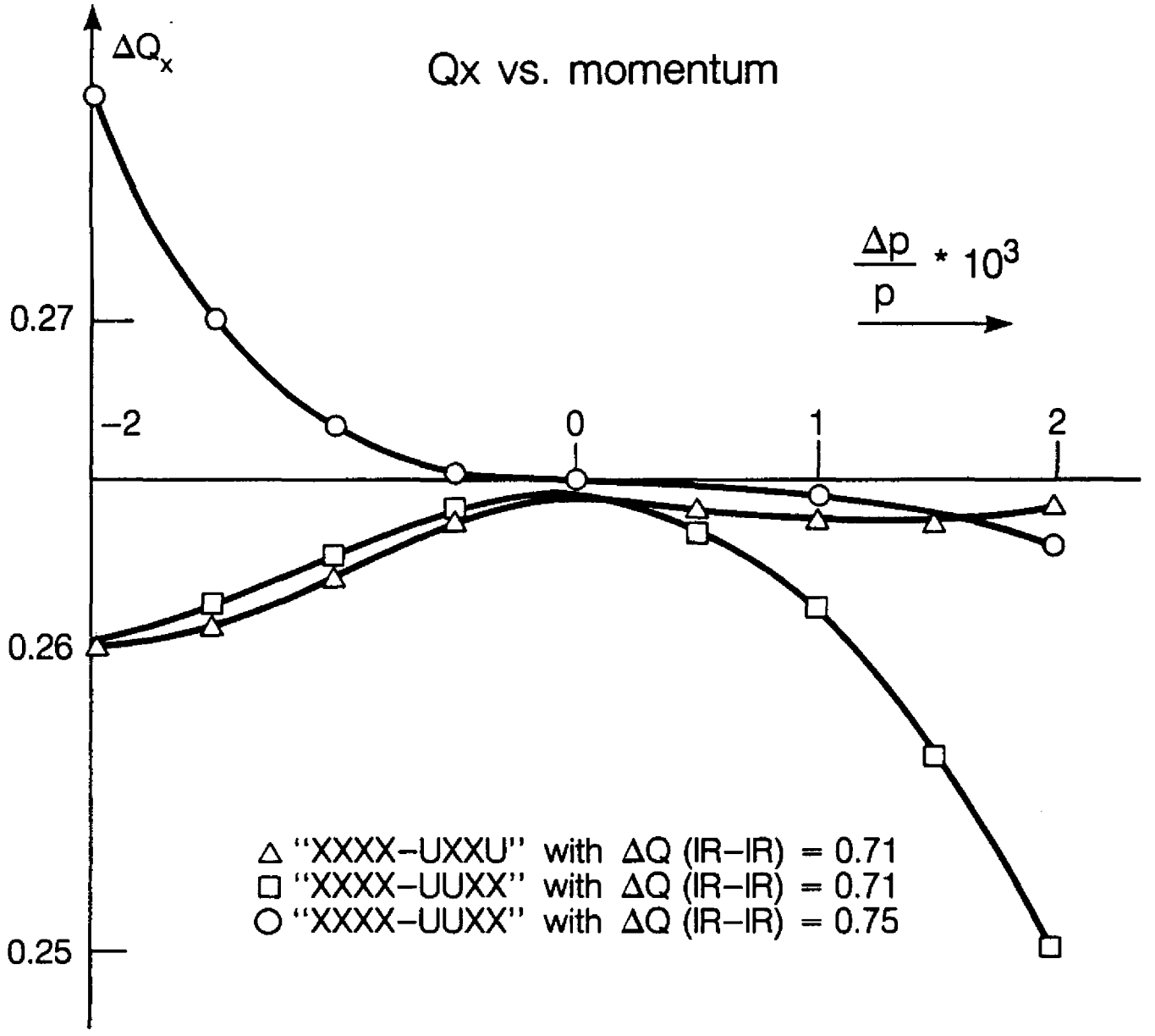

Figure 17. Q_x vs. Momentum

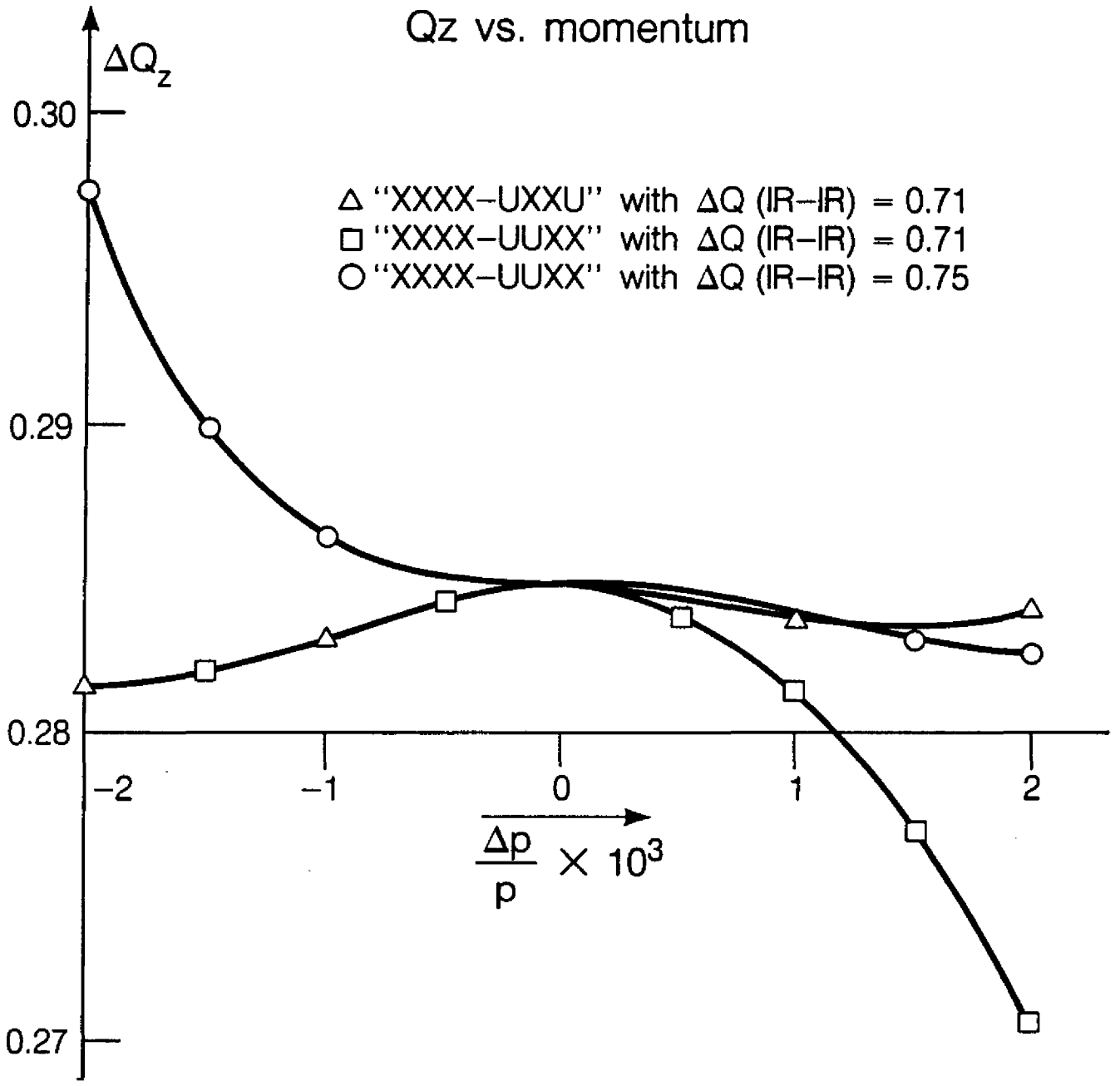

Figure 18. Q_z vs. Momentum

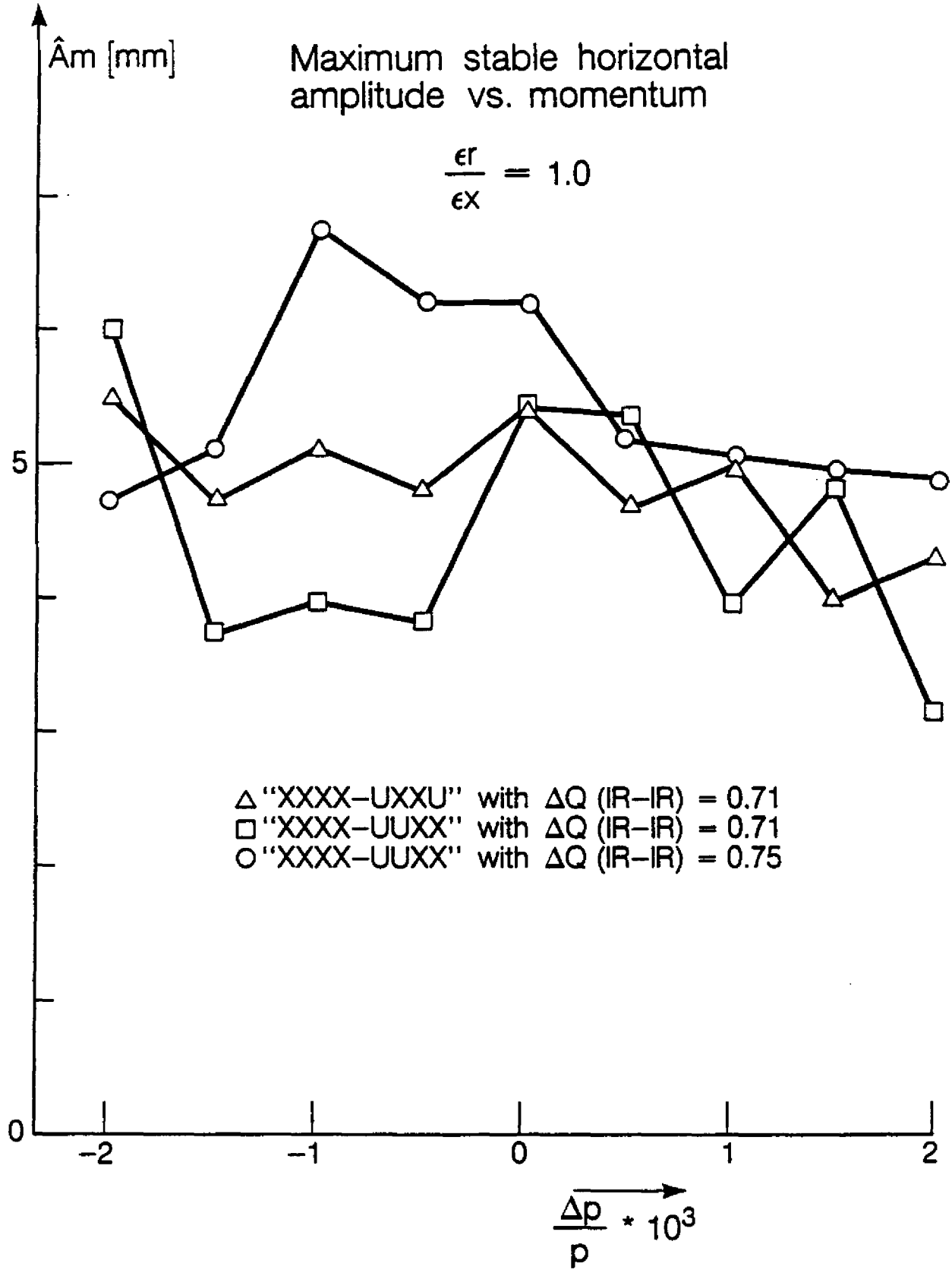

Figure 19. Maximum Stable Horizontal Amplitude vs. Momentum

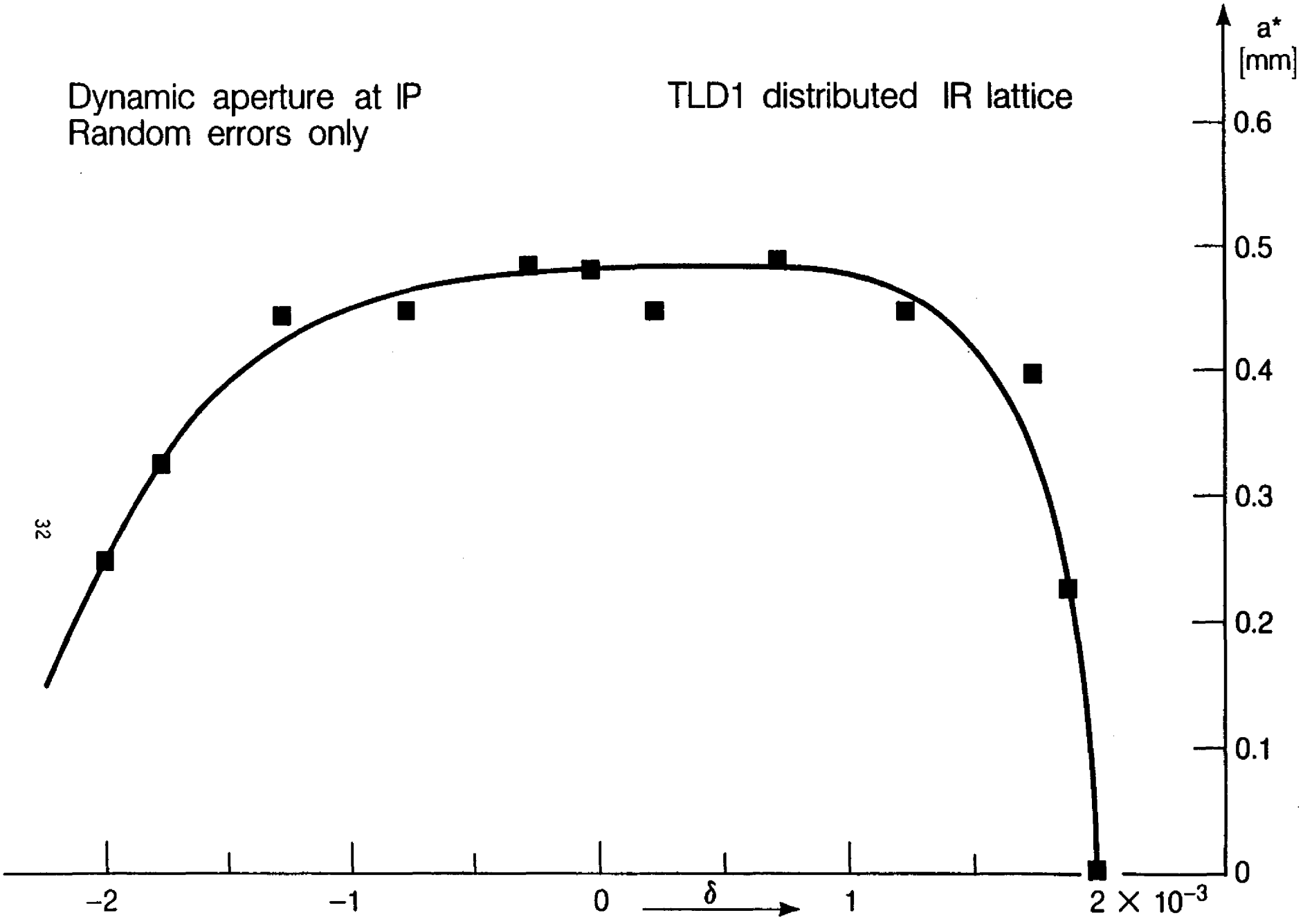

Figure 20. TLD1 Distributed IR Lattice

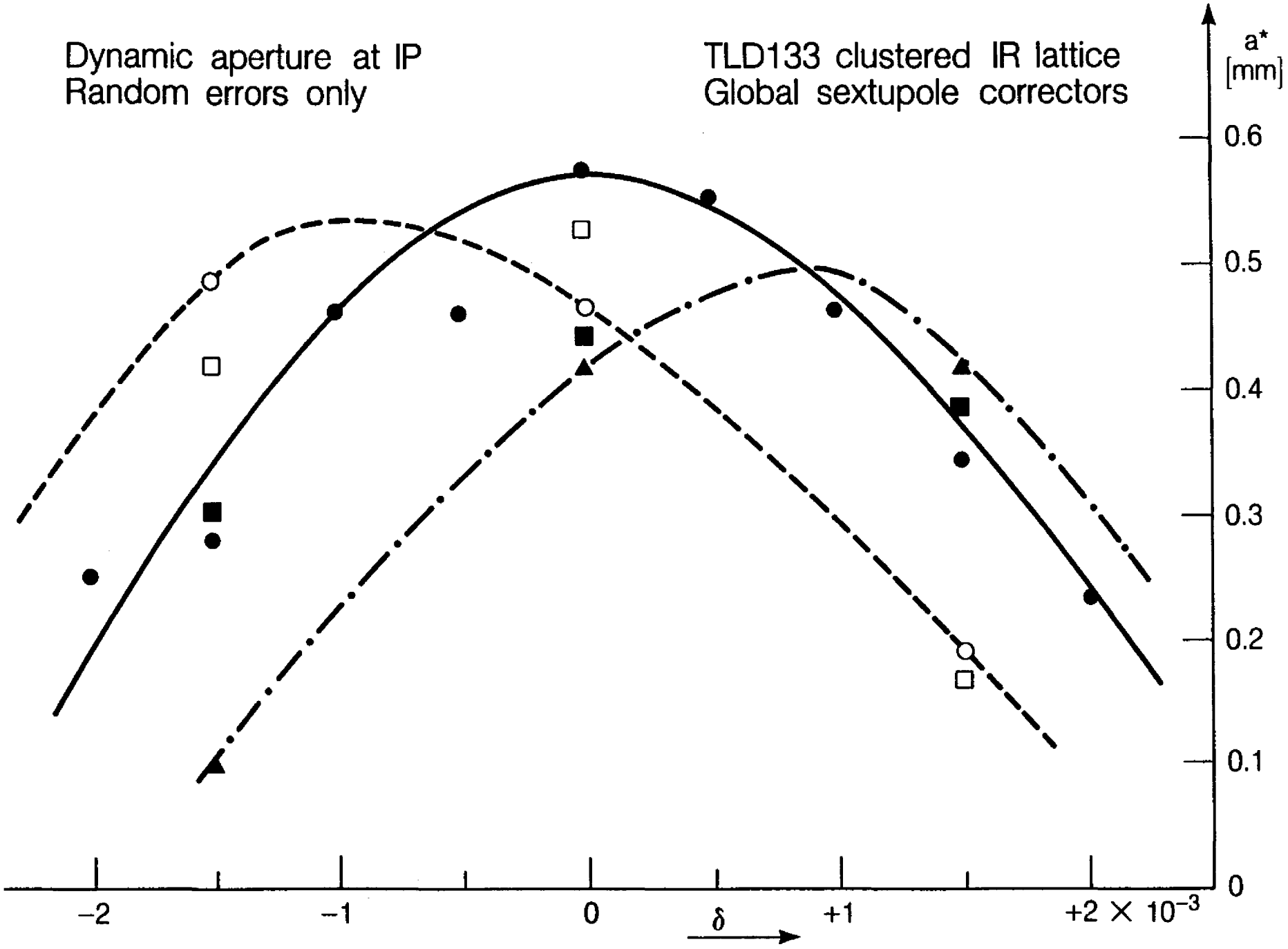

Figure 21. TLD133 Clustered IR Lattice Global Sextupole Correctors

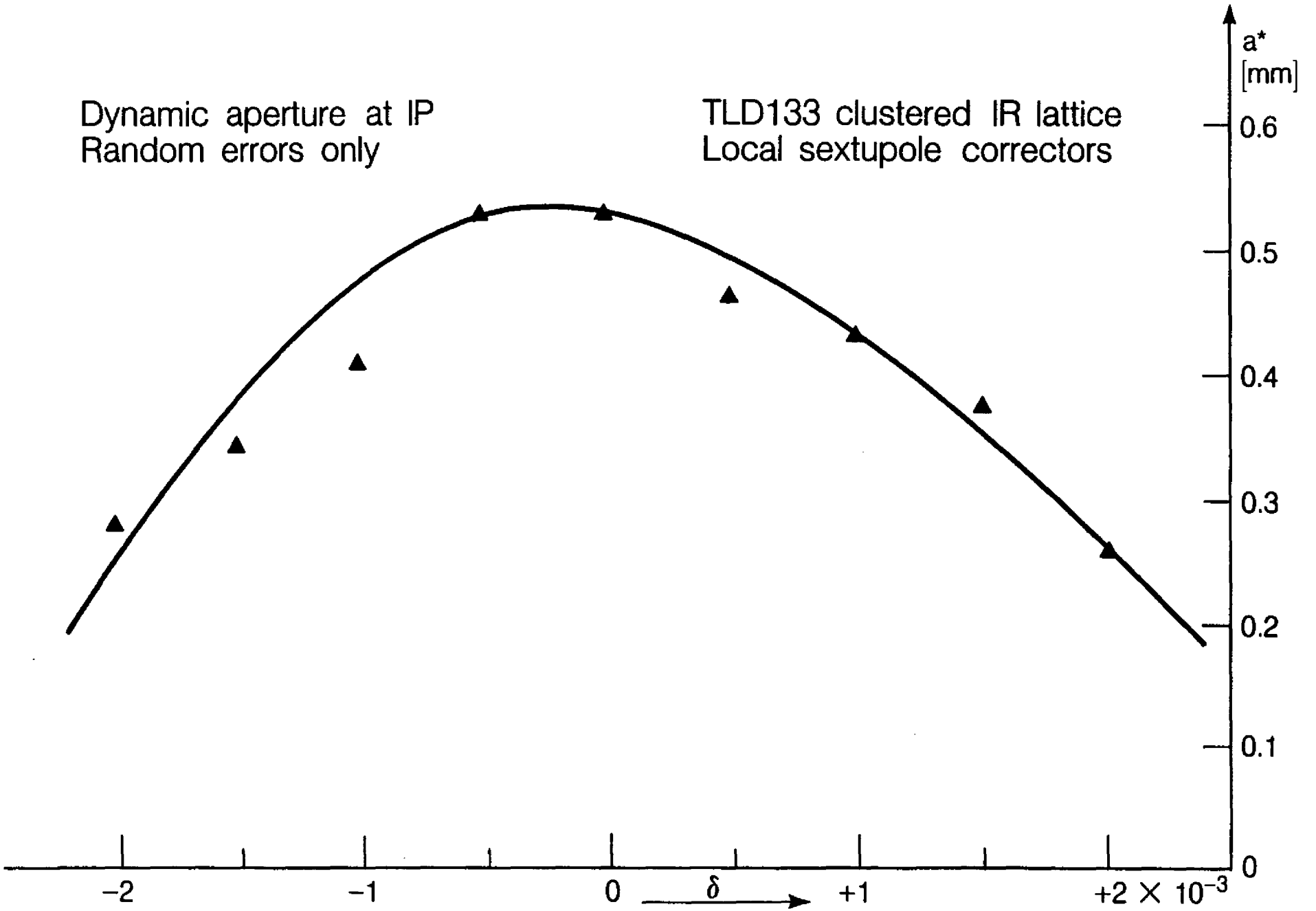

Figure 22. TLD133 Clustered IR Lattice Local Sextupole Correctors

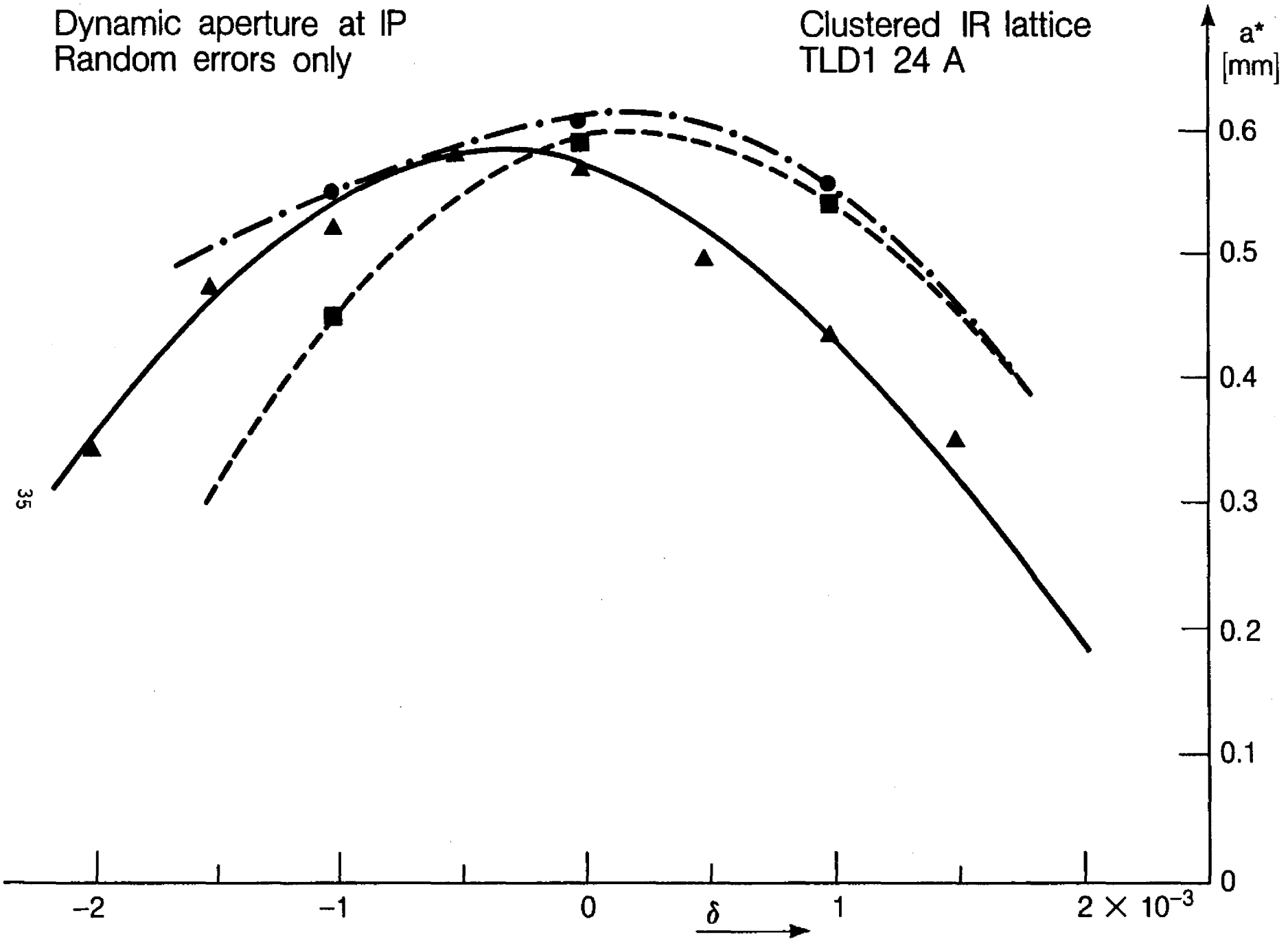

Figure 23. Clustered IR Lattice TLD124A

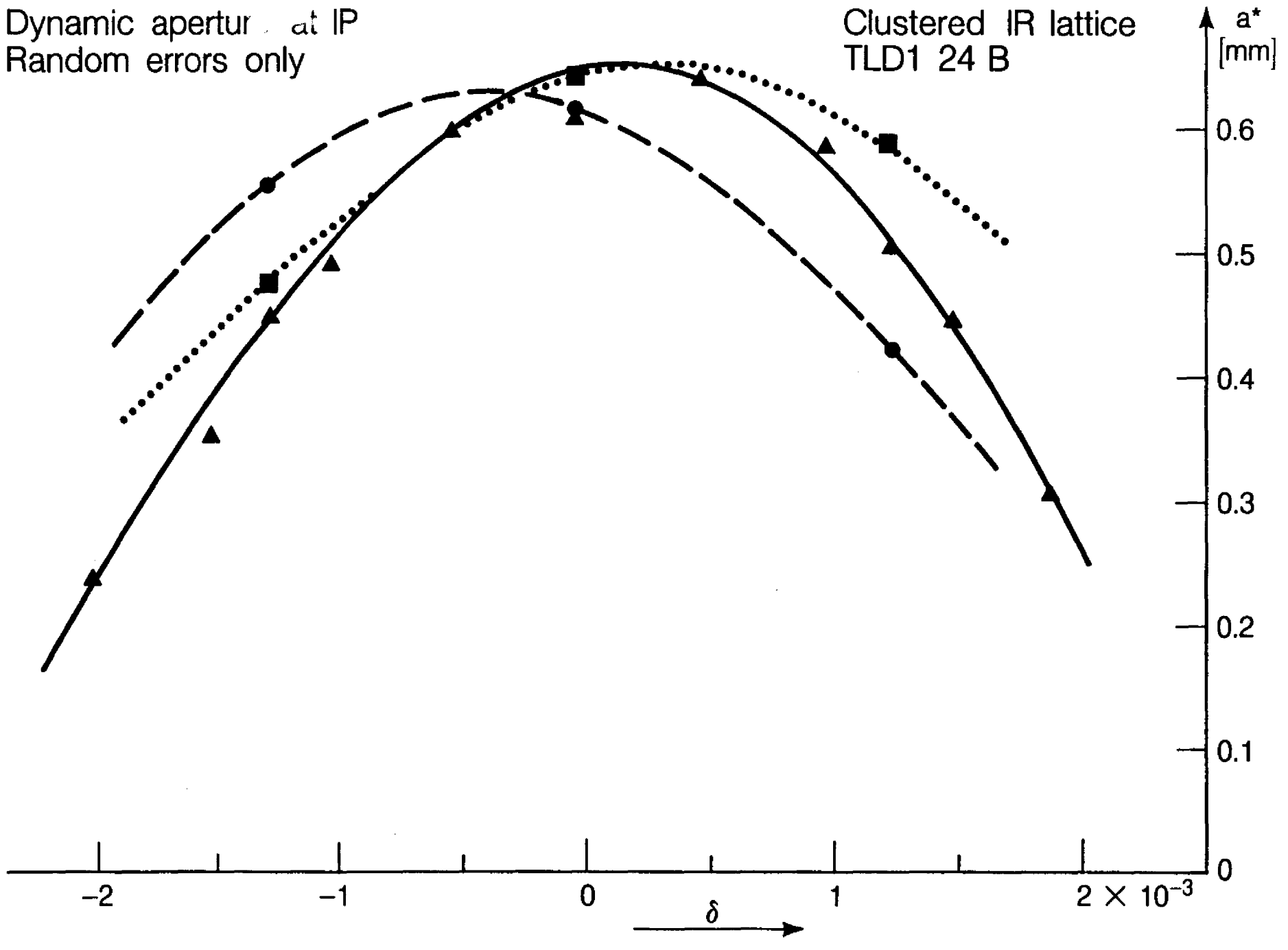

Figure 24. Clustered IR Lattice TLD124B